
Hyperfine Interactions **130:** 5–44, 2000.

Nanocrystalline materials – Current research and future directions

C. Suryanarayana [a] and C.C. Koch [b]

[a] *Department of Metallurgical and Materials Engineering, Colorado School of Mines, Golden, CO 80401-1887, USA*
[b] *Department of Materials Science and Engineering, North Carolina State University, Raleigh, NC 27695-7907, USA*

Nanocrystalline materials, with a grain size of typically < 100 nm, are a new class of materials with properties vastly different from and often superior to those of the conventional coarse-grained materials. These materials can be synthesized by a number of different techniques and the grain size, morphology, and composition can be controlled by controlling the process parameters. In comparison to the coarse-grained materials, nanocrystalline materials show higher strength and hardness, enhanced diffusivity, and superior soft and hard magnetic properties. Limited quantities of these materials are presently produced and marketed in the US, Canada, and elsewhere. Applications for these materials are being actively explored. The present article discusses the synthesis, structure, thermal stability, properties, and potential applications of nanocrystalline materials.

Keywords: nanocrystalline materials, synthesis, inert gas condensation, mechanical alloying, electrodeposition, crystallization of amorphous alloys, grain boundaries, thermal stability, grain growth, mechanical properties, magnetic properties, electrical properties, applications

1. Introduction

Nanocrystalline materials are single- or multi-phase polycrystalline solids with a grain size of a few nanometers (1 nm $= 10^{-9}$ m $= 10$ Å), typically less than 100 nm. Since the grain sizes are so small, a significant volume of the microstructure in nanocrystalline materials is composed of interfaces, mainly grain boundaries, i.e., a large volume fraction of the atoms resides in grain boundaries. Consequently, nanocrystalline materials exhibit properties that are significantly different from, and often improved over, their conventional coarse-grained polycrystalline counterparts [1]. Materials with microstructural features of nanometric dimensions are referred to in the literature as nanocrystalline materials (a very generic term), nanocrystals, nanostructured materials, nanophase materials, nanometer-sized crystalline solids, or solids with nanometer-sized microstructural features. Nanostructured solids is perhaps the most accurate description, even though nanocrystalline materials will be the appropriate term if one is dealing with solids with grains made up of crystals.

Nanocrystalline structures are not really very new. Nanocrystalline phases were detected in samples of lunar soils. Many conventional catalytic materials are based on very fine microstructures. Nanostructures formed chemically under ambient conditions can also be found in natural biological systems from seashells to bone and teeth in the human body. These materials are notable in that they are simultaneously hard, strong, and tough. Therefore, a number of investigations have been conducted to mimic nature (biomimetics) and also artificially synthesize nanostructured materials and study their properties and behavior. These investigations have clearly shown that one could engineer (tailor) the properties of nanocrystalline materials through control of microstructural features, more specifically the grain size.

Microstructural features on a nanometer-scale have been known to be useful in enhancing the properties and performance of materials. Early in the century, when "microstructures" were revealed primarily with the optical microscope, it was recognized that refined microstructures, for example, small grain sizes, often provided attractive properties such as increased strength and toughness in structural materials. A classic example of property enhancement due to a refined microstructure – with features too small to resolve with the optical microscope – was age hardening of aluminum alloys. The phenomenon, discovered by Alfred Wilm in 1906, was essentially explained by Merica, Waltenberg, and Scott in 1919, and the microstructural features responsible first inferred by the X-ray studies of Guinier and Preston in 1938. With the advent of transmission electron microscopy [2] and sophisticated X-ray diffraction methods [3] it is now known that the fine precipitates responsible for age hardening, e.g., in Al–4% Cu alloys are clusters of Cu atoms – GP zones – and the metastable partially coherent θ' precipitate. Maximum hardness is observed with a mixture of GPII (or θ'') (coarsened GP zones) and θ' with the dimensions of the θ' plates typically about 10 nm in thickness by 100 nm in diameter. Therefore, the important microstructural feature of age-hardened aluminum alloys is nanoscale. In recent years also there are a number of other examples of nanoscale microstructures providing optimized properties. The critical current density, J_c, of commercial superconducting Nb_3Sn is controlled by grain size, and is inversely proportional to grain size, with grain sizes of 50–80 nm providing high values of J_c [4]. Superhard and supertough materials are nanocomposites wherein about 10-nm-sized hard carbides (or other phases) are dispersed in an amorphous matrix [5].

Gleiter [6] and coworkers synthesized ultrafine-grained materials (with a grain size of a few nanometers) by the *in situ* consolidation of nanoscale atomic clusters in the 1980's and showed that these materials have properties significantly different from those of conventional grain sized (>1 μm) polycrystalline or amorphous materials of the same chemical composition. These results stimulated considerable research in this area and the field of nanocrystalline materials has now become a major identifiable activity in materials science.

The subject of nanocrystalline materials has attracted the attention of materials scientists, physicists, chemists, mechanical engineers, electrical engineers, and chemical engineers. This has led to both in-depth and broad-brush research activities on different aspects of nanocrystalline materials. A new journal entitled "NanoStructured Materi-

als" was launched in 1992 and continued till 1999. In addition to the Proceedings of a number of dedicated conferences and also as part of the activities of different societies such as MRS, TMS, and ASM International, the Proceedings of the annual ISMANAM (International Symposium on Metastable, Mechanically Alloyed, and Nanocrystalline Materials) and triennial RQ (Rapidly Quenched and Metastable Materials) series of conferences published in "Materials Science Forum" and in the international journal "Materials Science and Engineering A", respectively, constitute the best sources of information on different aspects of nanocrystalline materials.

The nanocrystalline materials pioneered by Gleiter were preceded by studies of nanoparticles by researchers such as Uyeda [7]. At present the very broad field of nanostructured materials includes (i) nanoparticles, (ii) nanocrystalline materials, and (iii) nanodevices. The potential applications for the various kinds of nanoscale materials include dispersions and coatings, high surface area materials, functional nanostructures (e.g., optoelectronic devices, biosensors, nanomachines) and bulk nanostructured materials for structural or magnetic applications.

Since a number of articles in this special volume will deal with the structural characterization of the defects present in nanocrystalline materials, this article will present an overview of the field with emphasis on the synthesis, structure, properties, and potential applications of nanocrystalline materials. The field of nanocrystalline materials has been reviewed earlier and the reader is referred to a number of recent review articles and conference proceedings [1,6,8–18] and also the references at the end of this article for details of the investigations, only briefly mentioned here. Thus we will highlight the current research and recent progress and indicate the future research directions in this exciting area. Even though it is impossible to completely discuss all the aspects of nanocrystalline materials, we will try to make this overview as self-contained as possible.

We will first classify the different types of nanostructured materials and follow this with a brief discussion of the important techniques available to synthesize them. We will then describe the structural features of the grains and grain boundaries in nanocrystalline materials. The properties and potential applications of these novel materials will then be described. We will conclude the article with the type of investigations required to further improving our understanding in this field. Efforts will be made to always compare the structure and properties of nanocrystalline materials with those of coarse-grained counterparts of the same chemical composition.

2. Classification

Nanocrystalline materials can be classified into different categories depending on the number of dimensions in which the material has nanometer modulations. Thus, they can be classified into (a) layered or lamellar structures, (b) filamentary structures, and (c) equiaxed nanostructured materials. A layered or lamellar structure is a one-dimensional (1D) nanostructure in which the magnitudes of length and width are much greater than the thickness that is only a few nanometers in size. One can also visualize

Table 1
Classification of nanocrystalline materials.

Dimensionality	Designation	Typical method(s) of synthesis
One-dimensional (1D)	Layered (lamellar)	Vapor deposition Electrodeposition
Two-dimensional (2D)	Filamentary	Chemical vapor deposition
Three-dimensional (3D)	Crystallites (equiaxed)	Gas condensation Mechanical alloying/milling

a two-dimensional (2D) rod-shaped nanostructure that can be termed filamentary and in this the length is substantially larger than width or diameter, which are of nanometer dimensions. The most common of the nanostructures, however, is basically equiaxed (all the three dimensions are of nanometer size) and are termed nanostructured crystallites (three-dimensional [3D] nanostructures) [19].

The nanostructured materials may contain crystalline, quasicrystalline, or amorphous phases and can be metals, ceramics, polymers, or composites. If the grains are made up of crystals, the material is called nanocrystalline. On the other hand, if they are made up of quasicrystalline or amorphous (glassy) phases, they are termed nanoquasicrystals and nanoglasses, respectively [1]. Gleiter [10] has further classified the nanostructured materials according to the composition, morphology, and distribution of the nanocrystalline component.

Table 1 shows this classification of the three types of nanostructures. Amongst the above, maximum research work is conducted on the synthesis, consolidation, and characterization of the 3D-nanostructured crystallites followed by the 1D-layered nanostructures. While the former are expected to find applications based on their high strength, improved formability, and a good combination of soft magnetic properties, the latter are targeted for electronic applications. Relatively few investigations have been carried out on the 2D-filamentary nanostructures.

3. Synthesis

Nanocrystalline materials can be synthesized either by consolidating small clusters or breaking down the bulk material into smaller and smaller dimensions. Gleiter [6] used the inert gas condensation technique to produce nanocrystalline powder particles and consolidated them *in situ* into small disks under ultra-high vacuum (UHV) conditions. Since then a number of techniques have been developed to prepare nanostructured materials starting from the vapor, liquid, or solid states. Table 2 lists some of the more common methods used to produce nanocrystalline materials and also the dimensionality of the product obtained. Nanostructured materials have been synthesized in recent years by methods including inert gas condensation, mechanical alloying, spray conversion processing, severe plastic deformation, electrodeposition, rapid solidification from

Table 2
Methods to synthesize nanocrystalline materials.

Starting phase	Technique	Dimensionality of product
Vapor	Inert gas condensation	3D
	Physical vapor deposition – Evaporation and sputtering	1D
	Plasma processing	3D
	Chemical vapor condensation	3D, 2D
	Chemical reactions	3D
Liquid	Rapid solidification	3D
	Electrodeposition	1D, 3D
	Chemical reactions	3D
Solid	Mechanical alloying/milling	3D
	Devitrification of amorphous phases	3D
	Spark erosion	3D
	Sliding wear	3D

the melt, physical vapor deposition, chemical vapor processing, co-precipitation, sol-gel processing, sliding wear, spark erosion, plasma processing, auto-ignition, laser ablation, hydrothermal pyrolysis, thermophoretic forced flux system, quenching the melt under high pressure, biological templating, sonochemical synthesis, and devitrification of amorphous phases. Actually, in practice any method capable of producing very fine grain-sized materials can be used to synthesize nanocrystalline materials. The grain size, morphology, and texture can be varied by suitably modifying/controlling the process variables in these methods. Each of these methods has advantages and disadvantages and one should choose the appropriate method depending upon the requirements. If a phase transformation is involved, e.g., liquid to solid or vapor to solid, then steps need to be taken to increase the nucleation rate and decrease the growth rate during formation of the product phase. In fact, it is this strategy that is used during devitrification of metallic glasses to produce nanocrystalline materials [20].

The choice of the method depends upon the ability to control the most important feature of the nanocrystalline materials, viz., the microstructural features (grain size, layer spacing, etc.). Other aspects of importance are the chemical composition and surface chemistry or cleanliness of the interfaces. Extremely clean interfaces can be produced and retained during processing and subsequent consolidation by conducting the experiments under UHV conditions; but, this adds up to the cost of processing. On the other hand, there are also methods that can be very inexpensive; but the purity of the product may not be high. Inert gas condensation, mechanical alloying/milling, spray conversion processing, electrodeposition, and devitrification of amorphous phases are some of the more popular techniques used to produce nanocrystalline materials.

3.1. Inert gas condensation

Vapor condensation has been known to produce very fine-grained or amorphous alloys depending on the substrate temperature and other operating conditions. Thus, this technique was originally used to synthesize small quantities of nanostructured pure metals. A number of variants have also been subsequently developed.

The inert gas condensation technique, popularized by Gleiter [6], consists of evaporating a metal (by resistive heating, radio-frequency heating, sputtering, electron beam heating, laser/plasma heating, or ion sputtering) inside a chamber that was evacuated to a very high vacuum of about 10^{-7} torr and then backfilled with a low pressure inert gas, typically a few hundred pascals of helium. The evaporated atoms collide with the gas atoms inside the chamber, lose their kinetic energy, and condense in the form of small, discrete crystals of loose powder. Convection currents, generated due to the heating of the inert gas by the evaporation source and cooled by the liquid nitrogen-filled collection device (cold finger), carry the condensed fine powders to the collector device, from where they can be stripped off by moving an annular teflon ring down the length of the tube into a compaction device. Compaction is carried out in a two-stage piston-and-anvil device initially at low pressures in the upper chamber to produce a loosely compacted pellet, which is then transferred in the vacuum system to a high-pressure unit where final compaction takes place. The scraping and compaction processes also are carried out under UHV conditions to maintain cleanliness of the particle surfaces (and subsequent interfaces) and also to minimize the amount of any trapped gases [8,21]. This process is used commercially to produce nanocrystalline oxide (and a few precious metal) powders by Nanophase Technologies Corporation in Burr Ridge, IL, USA.

The inert gas condensation method produces equiaxed (3D) crystallites. The crystal size of the powder is typically a few nanometers and the size distribution is narrow. The crystal size is dependent upon the inert gas pressure, the evaporation rate, and the gas composition. Extremely fine particles can be produced by decreasing either the gas pressure in the chamber or the evaporation rate and by using light (such as He) rather than heavy inert gases (such as Xe) [22].

Nanocrystalline alloys can be synthesized by evaporating the different metals from more than one evaporation source. Rotation of the cold finger helps in achieving a better mixing of the vapor. Oxides, nitrides, carbides, etc. of the metals can be synthesized by filling the chamber with oxygen or nitrogen gases or by maintaining a carbonaceous atmosphere. Additionally, at small enough particle sizes, metastable phases are also produced. Thus, this method allows the synthesis of a variety of nanocrystalline materials. High densities of as-compacted samples have been measured with values of about 75–90% of bulk density for metal samples.

A full description of the technique, the variety of evaporation methods, and the effect of process variables on the size, size distribution, and constitution of the powder particles can be found, for example, in [6,8,22]. Recently, a modified gas condensation technique has been used to synthesize Bi-coated copper crystallites [23]. Further, Chang et al. [24] modified the inert gas condensation apparatus by replacing the evaporative

source with a heated tubular reactor and using a metalorganic precursor instead of a pure metal. On heating, the metalorganic precursor decomposes to form a continuous stream of clusters or nanoparticles and these are entrained in a carrier gas. The nanoparticles condense out on a rotating liquid nitrogen cooled substrate from which the particles are scraped off and collected. Nanocrystalline SiC_xN_y and ZrO_xC_y powders were produced in this way. These particles were non-agglomerated and the process has high-rate production capabilities. It has also been reported that these powder particles can be sintered to theoretical density at temperatures as low as 0.5 T_m.

Sputtering, physical vapor deposition, plasma processing, and chemical vapor condensation techniques have also been employed to synthesize nanocrystalline materials. Details of these techniques may be found in [12].

3.2. Mechanical alloying

Mechanical alloying produces nanostructured materials by the structural disintegration of coarser-grained structure as a result of severe plastic deformation. Mechanical alloying consists of repeated welding, fracturing, and rewelding of powder particles in a dry high-energy ball mill until the composition of the resultant powder corresponds to the percentages of the respective constituents in the initial charge. In this process, mixtures of elemental or prealloyed powders are subjected to grinding under a protective atmosphere in equipment capable of high-energy compressive impact forces such as attrition mills, vibrating ball mills, and shaker mills. A majority of the work on nanocrystalline materials has been carried out in highly energetic small shaker mills. The process is referred to as mechanical *alloying* when one starts with a blended mixture of elemental powders and as mechanical *milling* when one starts with single component powders such as elements or intermetallic compounds. While material transfer is involved in mechanical alloying, no material transfer is involved in mechanical milling. These processes have produced nanocrystalline structures in pure metals, intermetallic compounds, and immiscible alloy systems. It has been shown that nanometer-sized grains can be obtained in almost any material after sufficient milling time. The grain sizes were found to decrease with milling time down to a minimum value that appeared to scale inversely with the melting temperature. Koch [25] and Suryanarayana [26] have recently summarized the process of mechanical alloying/milling and the characteristics and properties of the nanocrystalline materials thus obtained. Powder contamination (from the milling tools and/or the atmosphere) is usually a matter of concern with this process, especially when reactive metals and/or long milling times are involved; some remedial measures have been suggested in recent years [26].

In recent years, the process of severe plastic deformation of bulk solids (by the equal-channel-angular pressing, torsion straining, and accumulative roll bonding techniques) has been shown to produce ultrafine-grained structures. Even though the grain size is strictly not in the nanometer range (it is usually about 0.3–0.5 μm), there has been considerable amount of work on the structure and properties of materials produced

by these methods [27,28], essentially due to the possibility of producing bulk materials possessing submicron grain sizes.

3.3. Spray conversion processing

This is an industrial process employed by Nanodyne, Inc. (New Brunswick, NJ, USA) to produce nanocrystalline WC–Co composite powders. This process starts with aqueous solution precursors such as ammonium metatungstate [$(NH_4)_6(H_2W_{12}O_{40})\cdot 4H_2O$] and $CoCl_2$, [$Co(CH_3COO)_2$], or cobalt nitrate [$Co(NO_3)_2$]. The solution mixture is aerosolized and rapidly spray dried to give extremely fine mixtures of tungsten and cobalt complex compounds. This precursor powder is then reduced with hydrogen and reacted with carbon monoxide in a fluidized-bed reactor to yield nanophase cobalt/tungsten carbide powder. The tungsten particles are 20–40 nm in size. A typical powder particle consists of a hollow, porous 75 μm sphere containing hundreds of millions of WC grains in a cobalt matrix. To prevent grain growth of tungsten, additions of inhibitors such as VC and Cr_3C_2 are made as binders during the sintering steps. Recently, vanadium is being introduced into the starting solution itself to achieve a more uniform distribution in the powder mixture. The process parameters are being further optimized and since the process is fully integrated, on-line control is also being planned [29].

3.4. Electrodeposition

This is a simple and well-established process and can be easily adapted to produce nanocrystalline materials [30,31]. Electrodeposition of multilayered (1D) metals can be achieved using either two separate electrolytes or much more conveniently from one electrolyte by appropriate control of agitation and the electrical conditions (particularly voltage) [32]. Also, 3D nanostructure crystallites can be prepared using this method by utilizing the interference of one ion with the deposition of the other. Erb [30] and his collaborators have extensively used this process to study the synthesis and properties of 3D nanocrystalline materials. It has been shown that electrodeposition yields grain sizes in the nanometer range when the electrodeposition variables (e.g., bath composition, pH, temperature, current density, etc.) are chosen such that nucleation of new grains is favored rather than growth of existing grains. This was achieved by using high deposition rates, formation of appropriate complexes in the bath, addition of suitable surface-active elements to reduce surface diffusion of ad-atoms, etc. This technique can yield porosity-free finished products that do not require subsequent consolidation processing. Further, the process requires low initial capital investment and provides high production rates with few shape and size limitations. For these reasons, NanoMetals Corporation, London, Ontario, Canada is using this process for industrial applications [33].

3.5. Devitrification of amorphous phases

Many non-equilibrium processing techniques such as rapid solidification from the liquid state, mechanical alloying/milling, electrodeposition, and vapor deposition can produce amorphous (glassy) alloys. Controlled crystallization of these amorphous alloys (by increasing the rate of nucleation and decreasing the rate of growth) leads to the synthesis of nanostructured materials. In fact, the most common method to produce nanocrystalline magnetic materials has been to obtain an amorphous phase by rapidly solidifying the melt of appropriate composition and then crystallizing the glassy phase at a relatively low temperature. These materials – referred to as FINEMET – were first investigated by Yoshizawa et al. [34] and this technique has now become an established practice to study the structure and properties of nanocrystalline magnetic materials [20]. This simple devitrification method has been commonly employed to study the magnetic properties of nanocrystalline materials because it can produce (a) porosity-free samples, (b) samples with different grain sizes by controlling the crystallization parameters, and (c) large quantities of material. Furthermore, since no artificial consolidation process is involved (like in inert gas condensation, mechanical alloying, or plasma processing, where fine powders are produced), the interfaces are clean and the product is dense. Additionally, samples with different grain sizes can be synthesized by controlling the crystallization process, affording a way of comparing the properties of amorphous, nanocrystalline, and coarse-grained materials of the same composition [1,20].

In recent times there have been several basic investigations to define the conditions under which very fine (nanocrystalline) microstructures form starting from the glassy phases [35,36]. A recent development in this area is that nanocrystalline materials are produced by crystallization of amorphous powders or ribbons when they are subjected to mechanical milling [37]. Even though the exact mechanism of this process is presently not known, this offers a useful route to the preparation of high-purity nanocrystalline materials in bulk quantities since metallic glassy ribbons are commercially available.

All the above-mentioned methods produce equiaxed (3D) nanocrystallites. However, the 1D nanocrystalline materials (lamellar structures) are another important category and these are most commonly produced by the vapor deposition or electrodeposition methods. Bickerdike et al. [38] have described a semicommercial scale electron beam vapor deposition process which results in alternate layers of aluminum (20–1600 nm thick) and a second metal (0.1–20 nm thick Cr, Fe, Mg, Mn, Ni, or Ti). The vapor was condensed on a temperature-controlled disk-shaped aluminum alloy collector with a polished surface that can be rotated about a vertical axis. Deposits 160 mm in diameter were obtained at rates of 1–3 mm/h. Additionally, nanofibers, nanotubes, and nanorods are also being synthesized to be used as reinforcements to produce nanocomposites [39].

Several companies all over the world have started producing nanocrystalline powders on a commercial scale. According to a recent estimate [40], in the United States alone, over 50 small and large companies are active at various levels in the development

and production of nanocrystalline materials. More than a dozen of these businesses are involved in the manufacture of nanostructured materials on an industrial scale.

3.6. Consolidation of powder to bulk shapes

Widespread application of nanocrystalline materials requires production of the powder in tonnage quantities and also efficient methods of consolidating the powders into bulk shapes. The product of majority of the methods to synthesize nanocrystalline materials described above (with the exception of electrodeposition and devitrification of amorphous phases) is powder and therefore this needs to be consolidated. All the consolidation methods generally used in powder metallurgy processes can also be used for nanocrystalline materials. However, because of the small size of the powder particles (typically a few microns, even though the grain size is only a few nanometers), some special precautions need to be taken to minimize their chemical activity and also the high level of interparticle friction.

Successful consolidation of nanocrystalline powders is a non-trivial problem since fully dense materials should be produced while simultaneously retaining the nanometer-sized grains without coarsening. Conventional consolidation of powders to full density through processes such as hot extrusion and hot isostatic pressing requires use of high pressures and elevated temperatures for extended periods of time to achieve full densification. Unfortunately, however, this results in significant coarsening of the nanometer-sized grains and consequently the benefits of nanostructure processing are lost. On the other hand, retention of nanostructures requires use of low consolidation temperatures and it is difficult to achieve full inter-particle bonding at these low temperatures. Therefore, novel and innovative methods of consolidating nanocrystalline powders are required.

Successful consolidation of nanocrystalline powders has been achieved by electro-discharge compaction, plasma-activated sintering, shock (explosive) consolidation, hot-isostatic pressing (HIP), Ceracon processing (the Ceracon process (CERAmic CONsolidation) involves taking a heated preform and consolidating the material by pressure against a granular ceramic medium using a conventional forging press), hydrostatic extrusion, strained powder rolling, and sinter forging. By utilizing the combination of high temperature and pressure, HIP can achieve a particular density at lower pressure when compared to cold isostatic pressing or at lower temperature when compared to sintering. The results of some of these investigations are summarized [41–45]. It should be noted that because of the increased diffusivity in nanocrystalline materials, sintering (densification) takes place at temperatures much lower than in coarse-grained materials. This is likely to reduce the grain growth.

As we shall see later, nanocrystalline materials have been shown to exhibit increased strength/hardness, enhanced diffusivity, reduced density, higher electrical resistivity, increased specific heat, higher coefficient of thermal expansion, lower thermal conductivity, and superior soft magnetic properties in comparison to their coarse-grained counterparts. But, subsequent careful investigations on fully dense nanocrystalline ma-

terials, e.g., those produced by electrodeposition methods, have indicated that at least some of the "significant" changes in these properties could be attributed to the presence of porosity, cracks, and other discontinuities in the processed materials. Thus, it becomes important to obtain fully dense materials while simultaneously retaining nanometer-sized grains to unambiguously demonstrate the improvement in properties due to nanostructure processing.

4. Structure

Figure 1 shows a schematic representation of a hard-sphere model of an equiaxed nanocrystalline metal. Two types of atoms can be distinguished: crystal atoms with nearest neighbor configuration corresponding to the lattice and the boundary atoms with a variety of interatomic spacings, differing from boundary to boundary. A nanocrystalline metal contains typically a high number of interfaces ($\sim 6\times 10^{25}$ m^{-3} for a 10 nm-grain size) with random orientation relationships, and consequently, a substantial fraction of the atoms lies in the interfaces. Assuming, for simplicity, that grains have the shape of spheres or cubes, the volume fraction of nanocrystalline materials associated with the boundaries, C can be calculated as:

$$C = 3\Delta/d, \tag{1}$$

where Δ is the average grain boundary thickness and d is the average grain diameter. Thus, the volume fraction of atoms in the grain boundaries can be as much as 50% for 5-nm grains and decrease to about 30% for 10-nm grains and 3% for 100-nm grains. In contrast, for coarse-grained materials with a grain size of >1 μm, the volume fraction of atoms in the grain boundaries is negligibly small.

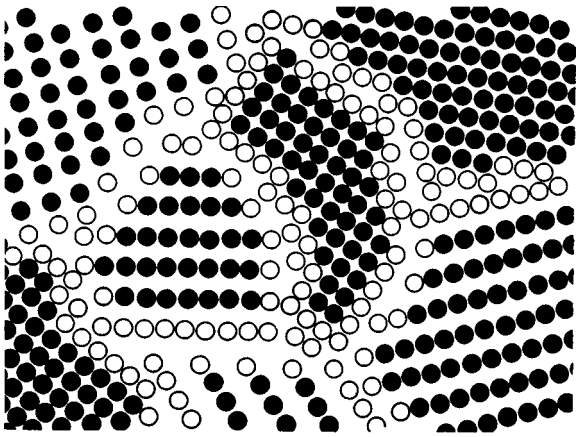

Figure 1. Schematic representation of an equiaxed nanocrystalline metal distinguishing between the atoms associated with the individual grains (filled circles) and those constituting the grain boundary network (open circles).

From the foregoing, it is clear that nanocrystalline metals can be considered to consist of two structural components – the numerous, small crystallites with long-range order and different crystallographic orientations constituting the "crystalline component" and a network of intercrystalline regions, the structure of which differs from region to region; this will be referred to as the "interfacial component". The interatomic spacings in the interfacial component have a wide distribution and further the average atomic density is considerably less than the crystal density depending on the type of chemical bonding between the atoms. Both these characteristics of the interfacial component (reduced density and wide distribution of interatomic spacings) have been confirmed by experimental observations using high-resolution electron microscopy, grazing incidence diffraction of X-rays, small-angle X-ray scattering, EXAFS (Extended X-ray Absorption Fine Structure), and other techniques.

4.1. Microstructure

In nanocrystalline single-phase alloys and pure metals, the most important structural parameter is the grain size. The properties of materials are mostly dependent on the grain size and therefore, an accurate determination of the grain size is important. Both direct (imaging) and indirect (scattering) techniques have been employed to determine the grain sizes.

Transmission electron microscopy (TEM) techniques (especially, the high-resolution TEM studies) are ideal to directly determine the grain sizes of nanocrystalline materials using the dark-field technique. The width of the Bragg reflection in an X-ray (large-angle) diffraction pattern can provide grain (or crystal, i.e., the size of the coherently diffracting domain) size information after the appropriate corrections (for instrumental and strain effects) are incorporated. The TEM techniques can clearly indicate whether there is a distribution of grain sizes and it is also possible to obtain a grain size histogram by measuring the grain sizes and counting the number of grains. On the other hand, the X-ray diffraction technique gives only the average crystal size and this value depends strongly on which function is used when averaging over the size distribution. A number of recent studies discuss the techniques for an accurate measurement of grain sizes and application of X-ray peak shape analysis techniques to nanocrystalline materials [46,47].

4.2. Atomic structure of the grains

The structure of the grains (crystallites) in nanocrystalline materials has been normally accepted to be the same as in a coarse-grained material. Consequently, there have not been many investigations into this aspect. High-resolution TEM experiments have indicated that nanocrystalline materials consist of small crystallites of different crystallographic orientations separated by grain boundaries. Even though not frequently reported, the grains contained a variety of crystalline defects such as dislocations, twin boundaries, multiple twins, and stacking faults.

Table 3
Lattice distortions in nanocrystalline phases obtained by crystallization of the amorphous materials.

Amorphous phase	Crystalline phase	Crystal structure	Maximum observed deviation, %				Ref.
			$\Delta a/a$	$\Delta c/c$	$\Delta V/V$	Grain size, nm	
Fe–Cu–Si–B	α-Fe(Si)	Bcc	0.295	–	–	27	[48]
	Fe_2B	BCTetragonal	0.216	−0.237		11	
Fe–Mo–Si–B	Fe_2B	BCTetragonal	0.22	−0.24		25	[49]
Ni	Ni	Fcc	0.76	–	2.03	6.4	[50]
Ni–P	Ni_3P	Tetragonal	0.37	−0.13	–	6	[49]
Se	Se	Trigonal	0.29	−0.19	0.36	8.4	[51]

Lu and co-workers [48–51] synthesized nanocrystalline materials by crystallizing the amorphous phases obtained by rapid solidification of the melt. They investigated the structure of the grains using X-ray diffraction and Mössbauer spectroscopy techniques. The change in lattice parameters was evaluated by measuring the lattice parameter in the nanocrystalline state (a) and comparing it with the standard lattice parameter (a_0) and evaluating the difference as $\Delta a = a - a_0$. The other lattice parameters and lattice volumes also were calculated in a similar way and the results are summarized in table 3. Even though the crystal structure remains the same in both the nanocrystalline and coarse-grained condition, in all the cases it was noted that the "a" parameter was always larger and the "c" parameter smaller in the nanocrystalline state. The unit cell volume always increased. Further, these values, which are relatively small, even though computer simulation experiments showed them to be between 4 and 10% [52], changed with a change in grain size. These lattice distortions have been explained on the basis of a supersaturation of the constituent elements and/or vacancies [49]. Similar results have not been reported by others either in the same systems or others. One must exercise caution in interpreting these results. It is now well established that the solid solubility of elements is usually higher in the nanocrystalline state than in the coarse-grained condition. This change in solid solubility can lead to changes in lattice parameter(s), even though this explanation may not be valid for pure metals. Similarly, a significant change in vacancy concentration (although the effect is not that easy to detect) can also affect the lattice parameter(s). In fact, results different from the above were also reported. While Cr has a bcc structure under equilibrium conditions, it had, in the nanocrystalline state, the A15 structure under high-purity conditions, and the bcc structure in presence of oxygen impurities [53]. Weismüller [54] has reported that the lattice parameters of nanocrystalline metals are not significantly different from those of coarse-grained materials. It has also been noted that nanocrystalline materials have large mean square lattice strains, which increased systematically with a decreasing grain size. This strain appears to depend on the thermal and mechanical history of the specimen, suggesting that at least part of the strain is not intrinsic to the nanocrystalline state [55].

4.3. Atomic structure of the grain boundaries

The structure of the grain boundaries has received a lot of attention and has been discussed extensively in the literature, especially to decide whether it is different in the nanocrystalline and coarse-grained materials of the same composition. The grain boundary structure determines the diffusivity, and consequently the rate of deformation by grain boundary diffusion (Coble creep) and the rates of sintering and grain growth. The conclusions differ and some believe that the structure is fundamentally different in both the types of materials while others believe that it is the same. The present status of the structure of grain boundaries in nanocrystalline materials can be found in some recent review articles [1,54–57].

Gleiter and co-workers [6,10] and others [58] studied the structure of nanocrystalline materials using a number of techniques and showed that the grain boundaries in nanocrystalline materials may be random, rather than possessing either the short-range or long-range order normally found in conventional coarse-grained materials. This randomness has been associated with either the local structure of individual boundaries or the structural co-ordination among boundaries [6]. It was also noted that the boundaries in the as-prepared nanocrystalline Pd are in a state with lower atomic short-range order than conventional grain boundaries in polycrystalline materials. The grain boundary free energy of as-prepared nanocrystalline Pd was also computed to be twice that of the relaxed state. EXAFS studies also indicated a much larger reduction in the atomic co-ordination numbers than that detected by X-ray studies, supporting the concept of wide disordered grain boundaries in nanocrystalline materials. A recent computer simulation study of grain boundaries in nanocrystalline materials [59] reported that (i) long-range periodicity is absent, (ii) grain boundary energy distribution is narrower than in bicrystals, (iii) grain boundaries are wider, but the width distribution is narrower than in bicrystals, and (iv) in the zeroth order, the grain boundaries are an isotropic, cement-like phase, a picture rather dissimilar from the structures found in glasses (which have short-range order) and that derived from bicrystal studies. Based on these results, it has been suggested that the grain boundaries in nanocrystalline materials are fundamentally different from those in conventional coarse-grained materials. All the properties of nanocrystalline materials were thus explained assuming that the material is a mixture of two components – perfect long-range ordered atomic arrangement in the grains and a random interfacial component. But, the details of the atomic structure of the grain boundaries in a given nanocrystalline material may vary as a function of the time-temperature history of the sample (crystal size and external pressures).

Based on the evidence from X-ray diffraction, EXAFS, Mössbauer spectroscopy, Raman spectroscopy, high-resolution TEM images, and computer simulations, Siegel [57] has shown that the grain boundary structure in nanocrystalline materials is similar to that in coarser-grained conventional material. Based on their high-resolution TEM studies, Horita et al. [60] also concluded that there was no evidence for a gas-like or widely diffuse structure in the grain boundaries of submicron grain size materials. Siegel [57] suggested that the atoms that constitute the grain boundary volume in nanocrystalline

materials have sufficient mobility during cluster consolidation to accommodate themselves into relatively low-energy configurations. The possible effects of high-resolution TEM specimen surfaces on the grain boundary structure further supported the reliability of such structural observations. He concluded that "indeed, the frequent lack of recognition of significant surface and porosity (and probably adsorbed impurity, as well) contributions to many of the surface-sensitive structural measurements on nanophase materials that have been used to deduce information about their grain boundary structures has undoubtedly exacerbated the problem of elucidating their nature".

From the above, it is apparent that the question of whether the structure of grain boundaries in nanocrystalline materials is basically different from the coarse-grained crystals is not answered clearly. Further and more local investigations are required to get a clearer picture of this aspect.

Direct evidence for an accurate determination of the structure of grain boundaries is difficult in view of the relaxation at surfaces; additional results from field-ion microscopy (FIM) and scanning tunneling microscopy (STM) may shed new light. Further, it would be useful to compare the structure of the grain boundaries in the same material using the same characterization technique, but produced by different methods to resolve some of the conflicting data available in the literature. Ping et al. [61] studied the microstructure of nanocrystalline materials obtained by two different techniques. The samples studied included Pd obtained by the inert gas condensation and Ti–Ni–Si and Fe–Mo–Si–B obtained by devitrification of the amorphous phases. They reported that much less defect structure was detected inside the crystals or interfaces in a devitrified sample than in an inert gas condensed and *in situ* consolidated samples. Although not clearly mentioned, this difference could be, at least partially, due to the much less porosity present in the devitrified sample. They have also reported that while both ordered and disordered regions and nanovoids were present in the grain boundaries of inert gas condensed palladium, the samples obtained by devitrification of Ti–Ni–Si and Fe–Mo–Si–B amorphous alloys have only ordered structures. However, this investigation does not provide clear evidence whether the structure of the boundaries is different in samples obtained by different techniques since the samples also are different.

5. Thermal stability

Grain growth occurs in polycrystalline materials to decrease the interfacial energy and hence the total energy of the system. Since nanocrystalline materials have a highly disordered large interfacial component (and therefore they are in a high-energy state), the driving force for grain growth is expected to be high. This driving force is proportional to the specific grain boundary area, and therefore it varies as the inverse of the grain size. Accurate grain growth studies in nanocrystalline materials are difficult since the grain size cannot be accurately determined. Some studies have been, however, conducted by measuring the grain size using direct electron microscopic techniques or estimated from the X-ray diffraction peak broadening values. Grain growth studies have also been conducted by measuring some macroscopic property as a function of temperature or

time that is sensitive to grain size, e.g., electrical resistivity, magnetic susceptibility, coefficient of thermal expansion, etc.

Knowledge of the thermal stability of nanocrystalline materials is important for both technological and scientific reasons. From a technological point of view, the thermal stability is important for consolidation of nanocrystalline powders without coarsening the microstructure. From a scientific point of view, it would be instructive to check whether the grain growth behavior in nanocrystalline materials is similar to that in coarse-grained materials. Further, knowledge of both the nucleation and grain growth rates is needed to design an appropriate heating schedule to obtain the desired nanometer grain size during devitrification of amorphous precursors.

Grain growth can also occur in nanocrystalline materials during consolidation of the powder, which requires exposure of the powder to high temperatures and pressures for extended periods of time. But, this has not been a serious concern in many cases [45].

The basic scientific question regarding grain growth of nanocrystalline materials, as for all phenomena for nanocrystalline materials, is whether the behavior involves "new physics" or is simply the expected grain size dependent behavior extrapolated to nanometer grain sizes.

Studies of isothermal grain growth kinetics can provide information on the microscopic mechanism of growth. Isothermal grain growth kinetics are frequently described by the equation:

$$d^n - d_0^n = Kt, \tag{2}$$

where d is the grain size at time t and a constant temperature T, d_0 is the initial grain size, K is a constant and n is the grain growth exponent (or $1/n$ is the time exponent). The activation energy for grain growth, Q can also be obtained from the equation:

$$K = K_0 \exp\left(\frac{-Q}{RT}\right), \tag{3}$$

where K_0 is a pre-exponential constant and R is the gas constant. Both Q and n are important parameters in describing the kinetics and mechanism of grain growth.

5.1. Grain growth exponent

The observed grain growth exponent in nanocrystalline materials has been found to vary from low values of 2 to as high a value as 10, different from the value of 2 deduced from the parabolic relationship for grain growth in coarse-grained materials. While the value of n was found to vary in different alloy systems, the general trend is for the time exponent $1/n$ to increase toward the ideal 0.5 with increasing normalized annealing temperature, T/T_m (figure 2). T_m is the melting or liquidus temperature of the given material. The data for conventional grain size (>5–10 μm) materials also exhibits trends similar to those for nanocrystalline materials. In fact, the ideal value of $n = 2$ has only been observed in high-purity elements such as Cd, Fe, and Sn at high values of T/T_m.

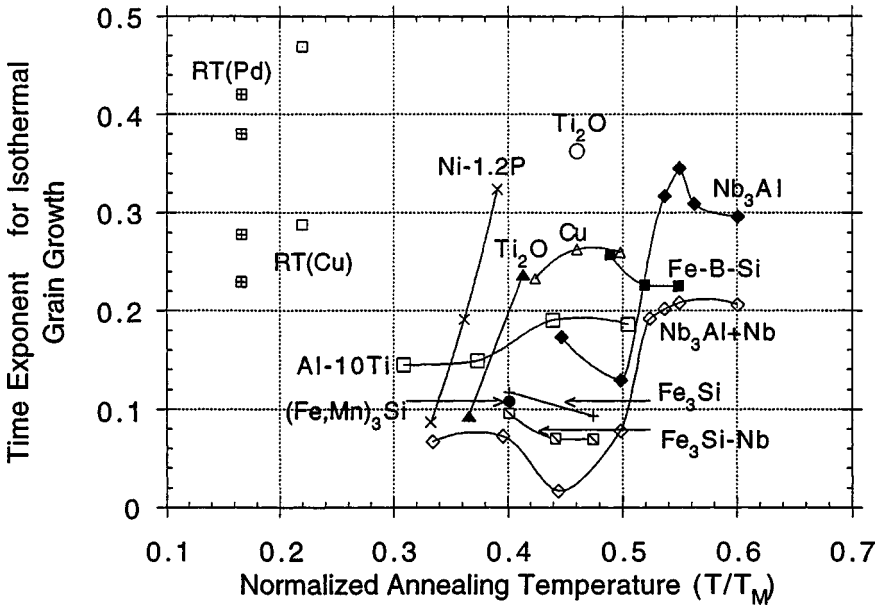

Figure 2. Time exponent, $1/n$, for isothermal grain growth of various nanocrystalline materials as a function of the reduced annealing temperature.

5.2. Activation energy for grain growth

Often the activation energy for grain growth is compared to the activation energy for lattice (Q_l) or grain boundary (Q_{gb}) diffusion in order to help determine the underlying mechanisms involved. Activation energy data for grain growth in nanocrystalline materials has been summarized in reference [62]. The data were compared to diffusion data; if the data does not exist, it was assumed that $Q_{gb} = 0.5Q_l$. Most of the results on Q for nanocrystalline materials compare better with Q_{gb} than with Q_l. This is consistent with most data for grain growth in conventional grain size materials. There are several exceptions to this general trend. In an Ag–7 at.% O alloy [63] oxidation of the Ag-powder led to an inhibition of grain growth by grain boundary pinning of an oxide phase. The peak temperature in the DSC scans shifted to a higher temperature by 60 K and the activation energy was found to have doubled, although abnormal grain growth was still found. Eckert et al. [64] found that the activation energy for grain growth in Pd compared closely to that of lattice self diffusion in Pd, while for Ni they found that the activation energy was close to that of grain boundary diffusion in Ni. The difference was attributed to a lower excess volume in Pd than in Ni that leads to a higher activation energy for grain growth in Pd.

The grain growth in nanocrystalline Fe was found to exhibit two regions of annealing temperature, i.e., $T > 500$°C and $T < 500$°C where the activation energies for grain growth are different [65]. The higher temperature region gave an activation energy of 248 kJ/mol which is comparable to that for grain growth in zone refined pure Fe with conventional grain sizes (>10 μm) and with Q_l for Fe. The lower temperature regime

yielded an activation energy of 125 kJ/mol that is lower than both Q_{gb} and Q_l for Fe. This suggests that grain growth in nanocrystalline Fe at $T > 500°C$ is similar to that in conventional grain size pure Fe, but grain growth in nanocrystalline Fe at $T < 500°C$ is due to another mechanism.

Depending on the alloy system under consideration, the activation energy for grain growth in nanocrystalline materials appears to be close to the value for lattice diffusion, grain boundary diffusion, or activation energy for crystallization of the amorphous phases [1,20].

5.3. Grain growth inhibition

A number of factors can influence grain boundary mobility and hence grain growth in nanocrystalline alloys. These include solute drag, pore drag, second phase (Zener) drag, and chemical ordering.

Contrary to expectations, experimental observations suggest that grain growth in nanocrystalline materials, prepared by any method, is very small (and almost negligible) up to a reasonably high temperature. It has been suggested that the resistance to grain growth observed in nanocrystalline materials results primarily from frustration, i.e., there is not sufficient driving force for grain growth [57]. This has been explained on the basis of structural factors such as narrow grain size distribution, equiaxed grain morphology, low energy grain boundary structures, relatively flat grain boundary configurations, and porosity present in the samples. In some instances, however, abnormal grain growth has been observed [66].

It has been observed in several systems that on heating a metastable nanocrystalline solid solution alloy, limited grain growth occurs while solute atoms also segregate to the grain boundaries. The grain boundary segregation then may lower the specific grain boundary energy sufficiently to reduce the driving force and limit further grain growth. This effect was illustrated clearly in $Pd_{1-x}Zr_x$ alloys [67] where $x = 0.1$ is an equilibrium solid solution and $x = 0.2$ is a metastable supersaturated solid solution. The 10 at.% Zr nanocrystalline alloy showed significant grain growth with an onset temperature of 325°C while the 20 at.% Zr nanocrystalline alloy had little or no grain growth at temperatures up to 500°C. While it is not possible to separate possible kinetic effects, such as solute drag, from this thermodynamic stabilization, the much slower grain growth in the 20 at.% Zr supersaturated alloy strongly suggests that the thermodynamic stabilization is dominant here. Solute segregation to nanocrystalline grain boundaries being responsible for grain size stabilization in supersaturated metastable nanocrystalline solid solutions has also been observed in some other alloys.

Pore drag has also been found to be operative in some materials. It has been shown that for an initial grain size of 14 nm in TiO_2, when the porosity was about 25%, the grain size after annealing for 20 h at 700°C was 30 nm. When the porosity was reduced to about 10%, the grain size for a similar annealing treatment was dramatically increased to 500 nm [68].

In conclusion it can be said that in order to learn about the mechanisms that govern the thermal stability/grain growth in nanocrystalline materials it is important to keep factors in mind that might interfere with grain growth. Specifically it would be desirable to avoid porosity, contamination and multiple phases (or precipitation) in future investigations.

6. Properties

Because of the very fine grain sizes and consequent high density of interfaces, nanocrystalline materials exhibit a variety of properties that are different and often considerably improved in comparison with those of conventional coarse-grained materials. These include increased strength/hardness, enhanced diffusivity, improved ductility/toughness, reduced density, reduced elastic modulus, higher electrical resistivity, increased specific heat, higher coefficient of thermal expansion, lower thermal conductivity, and superior soft magnetic properties. But, it is becoming increasingly clear that the early results on the properties of nanocrystalline materials are not very reliable, mainly due to the significant amount of porosity present in those samples. Thus, for example, the room temperature ductility in ceramic samples has not been reproduced. We will now try to summarize the properties of nanocrystalline materials and compare them with those of coarse-grained materials.

6.1. Diffusion and sinterability

Since nanocrystalline materials contain a very large fraction of atoms at the grain boundaries, the numerous interfaces provide a high density of short-circuit diffusion paths. Consequently, they are expected to exhibit an enhanced diffusivity in comparison to single crystals or conventional coarse-grained polycrystalline materials with the same chemical composition [69]. This enhanced diffusivity can have a significant effect on mechanical properties such as creep and superplasticity, ability to efficiently dope nanocrystalline materials with impurities at relatively low temperatures, and synthesis of alloy phases in immiscible metals and at temperatures much lower than those usually required for coarse-grained materials.

The measured diffusivities in nanocrystalline copper are about 14–20 orders of magnitude higher than lattice diffusion and about 2–4 orders of magnitude larger than grain boundary diffusion. For example, the measured diffusivity at room temperature is 2.6×10^{-20} m^2/s for 8 nm-grain sized copper samples compared to 4.8×10^{-24} for grain boundary diffusion and 4×10^{-40} for lattice diffusion [70]. Similarly enhanced diffusivities were also observed for solute diffusion in other metals. It may be mentioned in this context, that some investigators [71] ascribe this increased diffusivity to the presence of porosity in the consolidated samples. For example, if the presence of porosity is properly taken into account, the diffusivity of nanocrystalline materials has been found to be comparable to that of grain boundary diffusivity. The increased diffusivity (and

consequently the reactivity) leads to increased solid solubility limits (the solid solubility of Hg in nanocrystalline Cu has been reported to be 17 at.% against an equilibrium value of <l at.%) [72], formation of intermetallic phases (formation of Pd_3Bi at 120°C, a temperature much lower than normally required for coarse-grained materials) [73] and sometimes new phases, and increased sinterability of nanocrystalline powders.

The most important consequence of the increased diffusivity is that sintering of nanocrystalline powders can occur at temperatures much lower than those required for sintering coarse-grained polycrystalline powders. For example, TiO_2 with a grain size of 12 nm could be sintered at ambient pressures and at temperatures 400–600°C lower than that required for ball-milled 1.3 μm powder, and without the need for any compacting or sintering aids. Similarly nanocrystalline titanium aluminides can be fully consolidated at temperatures about 400°C lower than those required for coarse-grained materials [45].

Another consequence of the high diffusivity of nanocrystalline materials is that they are expected to show increased creep rate at low temperatures (see section 6.3 on mechanical properties). Although plastic deformation was reported to occur at room temperature in ceramics such as TiO_2 and CaF_2 [74] and large degree of deformation under compression in intermetallics such as Fe_3Al, these results have not been reproduced. The absence of extensive plastic deformation in fully dense nanocrystalline ceramic samples suggests that the plastic deformation observed earlier was probably due to the presence of porosity in the samples. The much-anticipated ductilization of inherently brittle ceramics and intermetallics has not been realized in practice. However, it has been recently reported that nanocrystalline NiAl prepared by inert gas condensation and consolidated to 90% of theoretical density with a grain size of 6 nm showed a strain to failure of 0.3% during biaxial disk bend testing [75]. This value should be compared with 0.02–0.06% for coarse-grained NiAl. This suggests that further densification to full density may increase the strain to failure even further and that diffusional creep may still be substantial in these materials.

6.2. Physical properties

6.2.1. Thermal expansion

Since nanocrystalline materials contain a large amount of interfacial volume, its coefficient of thermal expansion (CTE) is expected to be higher than in a coarse-grained material. Accordingly, measured values of CTE of nanocrystalline Cu, Pd, Fe–B–Si and Ni–P alloys were almost twice the value for single crystals [1]. For example, CTE for nanocrystalline (8 nm) Cu obtained by the inert gas condensation technique has been reported to be 31×10^{-6} K^{-1} in comparison with 16×10^{-6} K^{-1} for copper single crystals. Similar enhancements were observed in nanocrystalline Pd, Ni–P, $Fe_{78}B_{13}Si_9$ and TiO_2 samples (table 4).

Lu and Sui [76] measured the CTE of fully dense (porosity-free) nanocrystalline two-phase Ni–P samples of different grain sizes obtained by crystallizing the amorphous alloy at different temperatures. They reported that the CTE increased monotonically from 15.5×10^{-6} K^{-1} at a grain size of 127 nm to 20.7×10^{-6} K^{-1} for a grain size of

Table 4
Coefficients of thermal expansion (in 10^{-6} K^{-1}) of nanocrystalline, amorphous, and coarse-grained materials (after [1]).

Material	Temperature range (K)	Condition		
		Nanocrystalline	Amorphous	Coarse-grained
Ni–P	300–400	21.6	14.2	13.7
$Fe_{78}B_{13}Si_9$	300–500	14.1	7.4	6.9
Cu	110–293	31	–	16

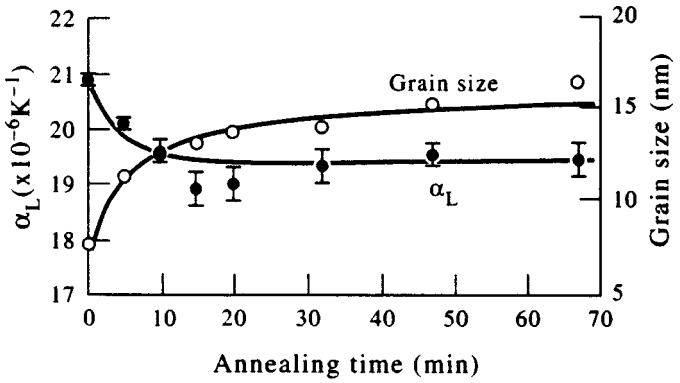

Figure 3. Variation of the average grain size and the coefficient of thermal expansion with annealing time for the nanocrystalline Ni–P sample annealed at 650 K. The initial nanocrystalline sample was prepared by completely crystallizing an amorphous Ni–P sample at 591 K for 13 min, average grain size 8 nm.

8 nm. The CTE decreased during grain growth (figure 3). From the dependence of CTE on grain size, they deduced that the difference in CTE between the interfaces and the nanometer-sized crystallites decreases when the grain size becomes smaller.

In contrast to these observations, it has been recently reported that the CTE of porosity-free electrodeposited nanocrystalline Ni was approximately the same as that of conventional polycrystalline Ni in the temperature range of 140–500 K [77]. Earlier observations have also noted that the difference in CTE between nanocrystalline and conventional materials depends strongly on the applied pressure during consolidation of gas-condensed powder. The general trend is that this difference decreases with increasing compaction pressure. Thus, recent observations suggest that there is no significant difference in the CTE of nanocrystalline and coarse-grained materials.

6.2.2. Specific heat

A comparison of the specific heats of different nanocrystalline, coarse-grained polycrystalline, and amorphous materials suggests that, at room temperature, the specific heat in the nanocrystalline state is much higher than that in the coarse-grained material and of even the amorphous material [1]. While most of the investigators reported a nonlinear (parabolic) variation of specific heat with temperature, some people

have reported a linear variation. It has also been noted that the specific heat increase at a constant temperature was linear with the reciprocal crystal size [78].

The large enhancement of the specific heat at room temperature and above is interpreted as the Einstein oscillator contribution due to weakly bound atoms at the interfaces of the nanocrystals. When the specific heat of 40 nm iron samples was measured at low temperatures (1.8–26 K), a quadratic temperature-dependent contribution to the heat capacity associated with surface modes was clearly observed. The electronic specific heat coefficient decreased by about 50%, suggesting the effect of increasing electron energy level spacing [79]. A small increase (2.5%) in specific heat was observed for porosity-free nanocrystalline Ni obtained by electrodeposition [77].

The specific heat of a material is closely related to its vibrational and configurational entropy, which is significantly affected by the nearest-neighbor configurations. Thus, the increase in specific heat of nanocrystalline materials has been attributed to the small crystal size (and consequent large interfacial component). If this is so, grain growth should reduce the specific heat of the nanocrystalline material. This was, in fact, observed [78].

6.2.3. Optical properties

The optical properties of nanocrystalline materials have been found to be exciting from both the scientific and technological points of view. The band gap of semiconductors and the optical transparency behavior of materials could be changed by controlling the grain and/or pore size in the nanocrystalline state. For example, the band gap in CdSe semiconductor could be changed from 3.0 eV for clusters of 1.2–1.5 nm to 2.3 eV for cluster sizes of 3.0–3.5 nm due to quantum confinement effects; the bulk material has a band gap of 1.8 eV [80]. By controlling the pore size in nanocrystalline Y_2O_3 to be equivalent to the wavelength of light, scattering could be effected and so the material was opaque. On the other hand, when the pore size was much smaller than the wavelength of light, scattering did not take place and so the material was fairly transparent [81]. The optical absorption characteristics can also be modified by allowing interaction to occur between the nanosized CdS clusters [82].

6.3. Mechanical properties

The mechanical behavior of nanostructured materials has been most recently reviewed by Morris [83] and so this topic will only be briefly covered here. It is to be noted that this is the least understood aspect of nanocrystalline materials.

6.3.1. Elastic properties

The elastic constants of nanocrystalline materials were found to be reduced by 30% [6], interpreted as due to the large free volume of the interfacial component and alternatively as due to the level of porosity and state of cracks present in the sample. Subsequent experiments on fully dense nanocrystalline materials, e.g., produced by electrodeposition, showed that the Young's modulus (E) of nanocrystalline Ni was compa-

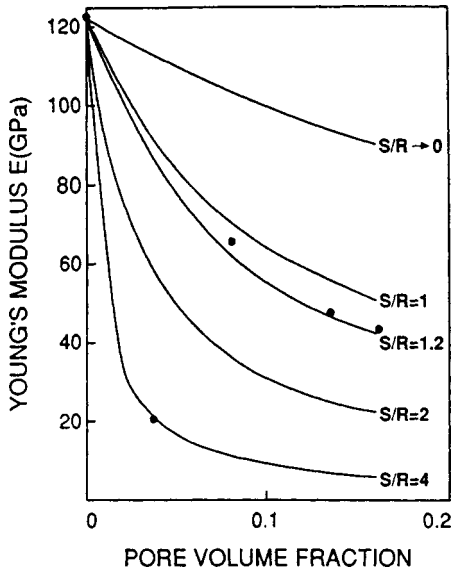

Figure 4. Calculated and measured Young's modulus for nanocrystalline Pd as a function of pore volume fraction for different S/R values.

rable to the coarse-grained sample [84]. It was also shown that the Young's moduli of 17–26 nm Cu, Ni, and Cu–Ni alloys produced by mechanical alloying techniques were essentially identical to those of the coarse-grained materials [85]. Thus, one should not expect any measurable difference in the E and shear modulus (G) of nanocrystalline and coarse-grained materials.

El-Sherik et al. [86] discussed the effects of porosity on E and magnetic properties and showed that the measured value of E can be significantly affected by the presence of porosity and cracks present in the consolidated material. For example, if the pore size is R and the flaw size emanating from the surface of the pore is S, then E of the compacted material is given by:

$$E = \frac{E_0}{1 + 4V\left(1 - \nu^2\right)\phi/\pi}, \tag{4}$$

where E_0 is the Young's modulus of the material without any porosity, V is the pore volume fraction, ν is the Poisson's ratio, and ϕ is a function of S and R. The variation of E with pore volume fraction for different values of S/R calculated using the above equation is presented in figure 4. It may be seen that the reduction can be as much as 80% depending upon the pore volume fraction and the ratio of S/R.

6.3.2. Strength and hardness

The most significant change resulting from a reduction in the grain size to the nanometer level is a 4–5 times increase in the strength and hardness over the coarse-grained material. The Hall–Petch relationship for conventional coarse-grained polycrys-

talline materials suggests that the yield strength (or hardness) of a material increases with a decreasing grain size according to the equation:

$$\sigma = \sigma_0 + K d^n, \tag{5}$$

where d is the mean grain size, σ is the 0.2% yield strength (or hardness), σ_0 is the lattice friction stress to move individual dislocations (or the hardness of a single crystal specimen), K is a constant, and n is the grain size exponent (generally $-1/2$). Even though the above relationship was obeyed by a number of nanocrystalline materials, some instances are also available when, below a critical grain size, the hardness was found to decrease with a decreasing grain size. That is, the slope K has a negative value and this has been termed as the inverse Hall–Petch relationship. Apart from the sign of K, there are also reports that the grain size exponent n can have very different values, e.g., -1, $-1/2$, $-1/3$, and $-1/4$. Some investigators have modified the normal Hall–Petch equation by modifying either the grain size exponent and/or the sign and magnitude of the slope K.

The Hall–Petch relationship was derived on the basis of strengthening resulting from dislocation pile-ups at physical obstacles like grain boundaries. Since nanocrystalline materials have extremely small grain sizes, Frank–Read sources may not be operating. Therefore, enough number of dislocations will not generate and migrate to have a pile-up, and so it is doubtful if strengthening could occur by this mechanism; other mechanisms may have to be invoked. While some people accept that the inverse Hall–Petch relationship is real and some theoretical explanations have been offered for its occurrence, others believe that this is an anomaly. When a high temperature for consolidation or annealing is used to increase the grain size, the size of flaws in the material could decrease or the density and/or the internal stresses in the compact could change and this could be the reason for the observed inverse Hall–Petch effect.

6.3.3. Ductility and toughness

It is well known that grain size has a strong effect on ductility and toughness of conventional grain size (>1 μm) materials. For example, the ductile/brittle transition temperature in mild steel can be lowered about 40°C by reducing the grain size by a factor of 5. Grain size refinement can make crack propagation more difficult and therefore increase the apparent fracture toughness in conventional grain size materials. However, the large increases in yield stress (hardness) observed in nanocrystalline materials suggests that fracture stress can be lower than yield stress and therefore result in reduced ductility. The results of ductility measurements on nanocrystalline metals are mixed and are sensitive to flaws and porosity, surface finish, and method of testing (e.g., tension vs. compression). But, as figure 5 clearly shows the elongation to failure has been found to decrease with a decrease in the grain size. Further, the ductility of nanocrystalline materials that exhibit ductile behavior with conventional grain sizes typically show reduced ductility – sometimes brittle behavior – at the smallest nanometer grain sizes. This is presumably due to the inability of usual dislocation generation and motion to occur at

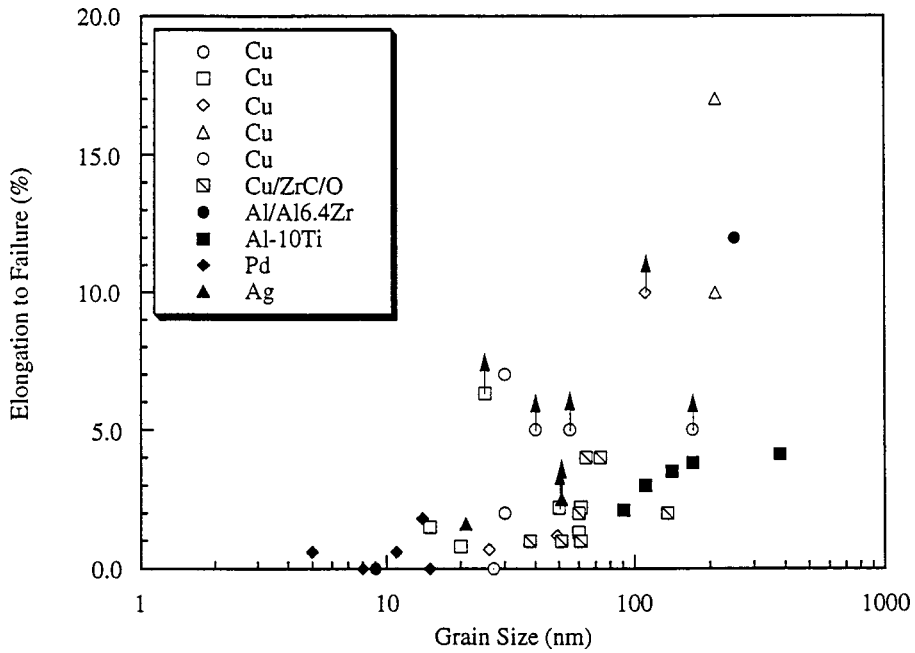

Figure 5. Elongation to failure in tension vs. grain size for some nanocrystalline metals and alloys.

these nanometer grain sizes. The question of ductility of nanostructured materials has been most recently addressed by Koch et al. [87].

It was shown that nanocrystalline ceramics, e.g., TiO_2 and CaF_2, could be plastically deformed at room temperature due to the increased creep rate as a result of grain boundary sliding due to a combination of fine grain size and increased grain boundary diffusivity [74]. An intriguing suggestion based on these early observations (not reproduced till date) is that the inherently brittle ceramics or intermetallics can be made ductile via nanostructure processing since the strain (creep) rate is given by:

$$\frac{\mathrm{d}\varepsilon}{\mathrm{d}t} = \frac{B\sigma\Omega\Delta D_\mathrm{b}}{d^3kT}, \tag{6}$$

where σ is the applied stress, Ω the atomic volume, Δ the grain boundary width, d the grain size, k the Boltzmann constant, T the temperature, B a constant and D_b the grain boundary diffusion coefficient. Decreasing the grain size from 1 μm to 10 nm should increase $\mathrm{d}\varepsilon/\mathrm{d}t$ by 10^6 or more if D_b is significantly larger for nanocrystalline materials. However, recent creep measurements of nanocrystalline Cu, Pd, and Al–Zr by Sanders et al. [88] at moderate temperatures find creep rates comparable to or lower than corresponding coarse-grain rates. However, there have not been reports for brittle ceramics or intermetallics of the dramatic increases in ductility predicted by eq. (6) at temperatures significantly $< 0.5T_\mathrm{m}$.

It has also been recently reported that very high strengths with acceptable levels of ductilites could be obtained in a material if about 20 vol% of a nanocrystalline phase is

uniformly dispersed in an amorphous matrix [89]. This appears to be a fruitful area for further investigations.

As grain size is decreased it is found that the temperature at which superplasticity occurs is lowered, and the strain rate for its occurrence is increased. According to eq. (6) the creep rates could be enhanced by many orders of magnitude and superplastic behavior might be observed in nanocrystalline materials at temperatures much lower than $0.5T_{\mathrm{m}}$.

Recently McFadden et al. [90] observed tensile superplasticity in nanocrystalline nickel obtained by electrodeposition and nickel aluminide obtained by severe plastic deformation. They reported that nickel exhibited superplasticity at 350°C, which is only $0.38T_{\mathrm{m}}$ and 470°C below the previous example of superplasticity in nickel. The initial grain size was of nanometer dimensions with a few larger (0.3 μm size) grains and grain growth occurred during the tensile test at 350°C up to about a micron. Strain hardening was also observed which was not reported for nanocrystalline materials at ambient temperature.

6.3.4. Deformation mechanisms

While there is still limited data on the mechanical behavior – especially tensile properties – of nanocrystalline materials, some generalizations may be made regarding the deformation mechanisms. It is likely that for the larger end of the nanoscale grain sizes, about 50–100 nm, dislocation activity dominates for test temperatures $<0.5T_{\mathrm{m}}$. As grain size decreases, dislocation activity apparently decreases. The essential lack of dislocations is presumably the result of the image forces that act on dislocations near surfaces or interfaces. The creation of new dislocations is also made difficult as the grain size reaches the lower end of the nanoscale ($\leqslant$10 nm). Thus at the smallest grain sizes we may have new phenomena controlling deformation behavior. It has been suggested that such phenomena [91] may involve grain boundary sliding and/or grain rotation accompanied by short-range diffusion assisted healing events.

The existing data on mechanical properties provide the following tentative conclusions, although much work remains to be done to clarify the detailed deformation mechanisms.

- Except for very small grain nanocrystalline samples ($\leqslant$5 nm) the elastic properties are essentially identical to those of coarse-grained material.
- High hardnesses and yield strength values are observed for nanocrystalline materials.
- Ductile coarse-grained materials are less ductile, perhaps brittle as nanocrystalline materials.
- Brittle coarse-grained materials may exhibit slight ductility when nanocrystalline. Not enough evidence to verify this.
- Superplasticity has been observed at low temperatures ($0.38T_{\mathrm{m}}$) for nanocrystalline nickel and nickel aluminide samples.

Table 5
Electrical resistivity of nanocrystalline materials.

Material	Grain size, nm	Room temperature resistivity $\mu\Omega$-cm	Temperature coefficient of resistivity, K^{-1}	Ref.
Ni–P	11	360	1.26×10^{-3}	[92]
	51	220	2.00×10^{-3}	
	102	200	2.35×10^{-3}	
$(Fe_{99}Cu_1)_{78}Si_9B_{13}$	30	126	2.01×10^{-3}	[93]
	50	60	1.6×10^{-3}	
	90	44	1.6×10^{-3}	
$(Fe_{99}Mo_1)_{78}Si_9B_{13}$	15	198	–	[94]
	200	63	–	

- Shear banding and perfectly plastic behavior have been seen in some nanocrystalline materials analogous to plastic deformation in amorphous materials.
- Mechanical twinning may be an alternate deformation mechanism in nanocrystalline materials.

6.4. Electrical properties

Because of the increased volume fraction of atoms lying at the grain boundaries, the electrical resistivity of nanocrystalline materials, as affected by grain boundary scattering, is found to be higher than that in the coarse-grained material of the same chemical composition (table 5). It has also been shown that the electrical resistivity of nanocrystalline materials is sensitive not only to the grain boundaries but also other types of imperfections and/or stresses introduced by the synthesis process [31]. At a constant temperature, the electrical resistivity increases with a decrease in grain size and for a constant grain size, the electrical resistivity increases with temperature, and both these observations are consistent with the theoretical analysis of scattering of electrons by grain boundaries.

The magnitude of the electrical resistivity (and hence conductivity) in nanocomposites can be changed by altering the grain size of the electrically conducting component. For example, by changing the volume fraction of iron particles in a nanocrystalline iron–silica system, the electrical conductivity could be changed by 14 orders of magnitude.

It has been recently reported that pure nanocrystalline ZnO with a 60 nm grain size can exhibit varistor behavior (constant voltage over a wide range of current) with a small, but usable threshold voltage of 0.1 kV/cm [95]. Further, by doping 3–10 nm ZnO with elements like B, Bi, Co, Cu, Sb, and Sn the varistor active range could be extended to 30 kV/cm [96], affording a means of controlling the voltages between 0.1 and 30 kV/cm by choosing the appropriate dopant.

The phenomenon of giant magnetoresistance (GMR) – drastic decrease of electrical resistivity of materials when exposed to a magnetic field – has been reported in a number of nanocrystalline multilayer and equiaxed systems [97]. Whereas the resistance drop is of the order of 1–2% in conventional materials, the drop in nanocrystalline materials could be as much as 50% or more. Nanostructured materials should be important in magnetic recording applications as new materials are developed with a stable, large GMR effect at room temperature that can operate at magnetic fields as low as a few mT.

6.5. Magnetic properties

Changes in the magnetic properties of nanoscale ferromagnetic materials can be attributed to their small volume, which means that they are typically single domain, and to the large fraction of atoms associated with the grain boundaries/interfaces. If the grain sizes are small enough, the structural distortions associated with the surfaces or interfaces can lower the Curie temperature, T_c, and reduce the magnitude of the saturation magnetization M_s. For example, the M_s of 6 nm Fe was reported to be 130 emu/g [6] compared to 220 emu/g for normal polycrystalline Fe. The Curie temperature of 10 nm Gd was decreased about 10 K from that of coarse-grained Gd, and the transition was broader [98]. These reductions were attributed to the deviation of interatomic spacings in the interfacial regions as compared with the crystalline component, supported by Mössbauer spectroscopy measurements. Such reductions were, however, not observed in fully dense electrodeposited nanocrystalline Ni [86,99] suggesting that the earlier results were influenced by the presence of porosity in the samples.

Attractive magnetic properties have been reported for nanocrystalline Fe-based alloys obtained by devitrification (at temperatures between 500 and 600°C) of the amorphous ribbon produced by the rapid solidification method [100]. The best soft magnetic properties by this route were obtained by the addition of Cu and at least one element selected from the group consisting of Nb, W, Ta, Zr, Hf, Ti, and Mo to an iron-base alloy having an essential composition $Fe_{74.5-x}Cu_xNb_3Si_{13.5}B_9$. These FINEMET alloys contain 10–15 nm-sized bcc Fe–Si grains embedded in the amorphous matrix. Small Cu-enriched particles have been found in the intergranular regions (figure 6).

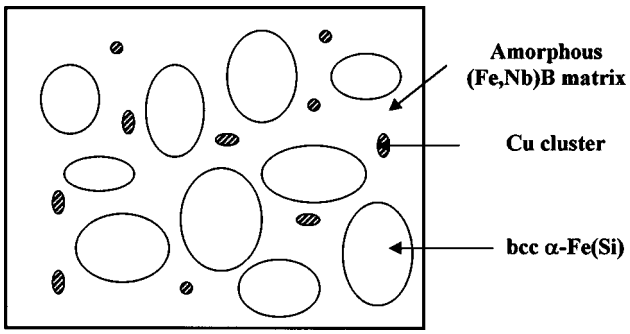

Figure 6. Schematic of the microstructure of FINEMET Fe–Cu–Nb–Si–B alloy.

Nanocrystalline materials produced by the crystallization of amorphous alloys (FINEMET alloys) show an excellent combination of magnetic characteristics. They have a low coercivity (5–10 A cm^{-1}), high permeability (100, 000), almost zero magnetostriction (0–2 $\times$ 10^{-6}), and low core losses ($\sim$200 kW m^{-3}) due to the high resistivity (135 $\mu\Omega$-cm) of these alloys. Further, the shape of the hysteresis loop can be altered by magnetic field annealing. All the above characteristics, in combination with good thermal stability, suggest that nanocrystalline Fe-based alloys are very promising candidates for soft-magnetic applications. The magnetic properties of these materials depend on the grain size, and hence on the temperature used for the crystallization. By changing the grain size, the coercivity can be changed by several orders of magnitude. The initial permeability also varied in a similar manner, essentially being inversely proportional to coercivity.

Due to the relatively low Fe content, the FINEMET alloys have a B_s less than 1.4 T. It is desirable to have soft magnetic materials with $B_s > 1.5$ T and μ_e above 10^5 at 1 kHz for various kinds of power transformers. Higher Fe content amorphous alloys of type Fe–M–B (M = Zr, Hf, or Nb) were subsequently studied and mixed phase nanocrystalline/amorphous structures were found to exhibit excellent soft magnetic properties [101]. These alloys (the "Nanoperm" family) developed by the Alps Electric Co. of Japan are typified by a composition such as $Fe_{86}Zr_7B_6Cu_1$. The addition of Cu aids in increased nucleation while Zr acts to inhibit growth (as well as allowing for amorphization). The core losses for this material are compared to those for conventional coarse-grained Fe–3.5% Si and amorphous Fe–9% Si–13% B in figure 7. The mechanism proposed for the good soft magnetic properties for the nanoscale bcc Fe–M–B alloys is believed to be due to the following factors:

- a high B_s resulting from the increased Fe content and the magnetic coupling between the nanoscale bcc particles via the ferromagnetic amorphous phase,
- the reversible magnetization due to magnetic homogeneity from the nanocrystalline bcc Fe phase being smaller than the width of magnetic domain walls,
- the stability of the nanocrystalline structure enhanced by the enrichment of solute elements in the amorphous phase,
- the reduction of the saturated magnetostriction, λ_s, resulting from the redistribution of the solute elements between the nanocrystalline bcc and amorphous phases.

The addition of Co to these alloys can enhance the values of B_s and μ_e [99] and balancing additions of Zr and Nb can achieve nearly zero λ_s.

The first attempts to produce nanoscale microstructures to enhance the magnetic properties of the Nd–Fe–B permanent magnetic materials used mechanical alloying of blended elemental powders followed by heat treatment [103]. Since the grain structure so obtained does not exhibit any crystallographic texture – and limits the energy product – special processing methods such as die-upsetting were needed to provide the crystallographic anisotropy. While the coercivities of these nanocrystalline alloys are high, the remanent magnetization is decreased.

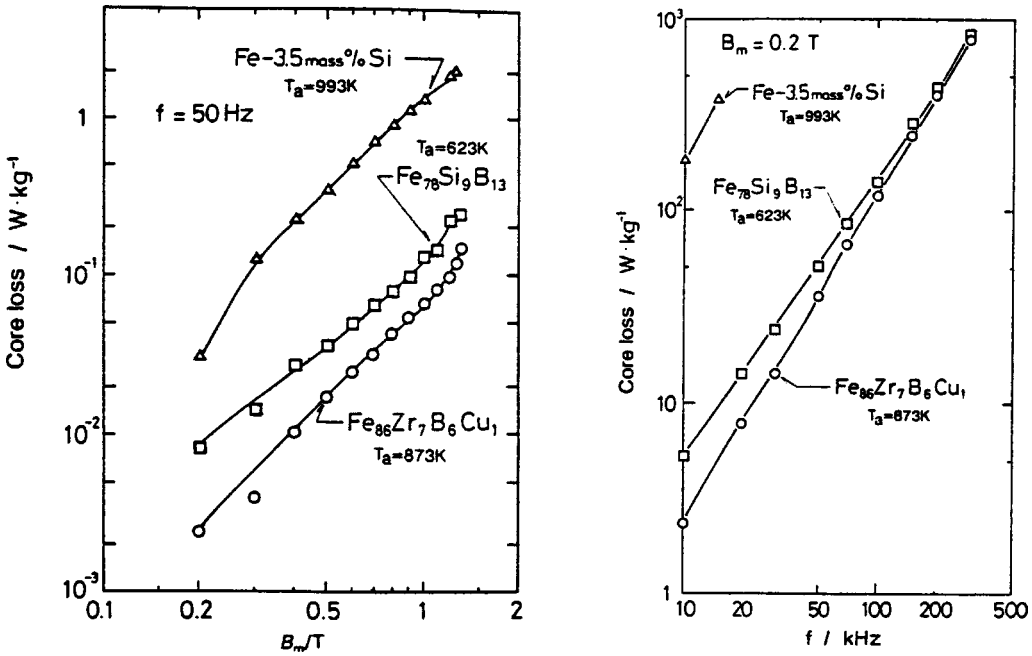

Figure 7. Comparison of core losses of conventional coarse-grained Fe–3.5 wt% Si, amorphous Fe–9 at.% Si–13 at.%B, and nanocrystalline Fe–7 at.% Zr–6 at.% B–1 at.% Cu alloys as a function of maximum induction field B_m and frequency f. T_a is annealing temperature.

Recent approaches to increase the magnetic induction have utilized exchange coupling in magnetically hard and soft phases. The Fe-rich compositions (e.g., $Fe_{90}Nd_7B_3$) result in a mixture of the hard $Fe_{14}Nd_2B$ phase and soft α-Fe phase. The nanoscale two-phase mixtures of a hard magnetic phase and a soft magnetic phase can exhibit values of remanent magnetization, M_r, significantly greater than the isotropic value of $0.5M_s$. This "remanence enhancement" is associated with exchange coupling between the hard and soft phases which forces the magnetization vector of the soft phase to be rotated to that of the hard phase [104].

While both rapid solidification from the melt and mechanical alloying techniques have been used widely to produce nanocrystalline magnetic alloys, the process parameters can be more easily and accurately controlled in the rapid solidification processing. Mechanical alloying seems to be unsuitable for the production of soft magnetic low coercivity alloys, because of the significant introduction of internal strain into the highly magnetostrictive material. Strain removal by annealing leads to undesirable grain growth. Thus, crystallization of amorphous alloys appears to be the best method to synthesize nanocrystalline alloys with attractive soft magnetic properties.

A useful magnetic property that nanocomposites offer is called the magnetocaloric effect. When a material containing extremely small magnetic particulates in a non-magnetic or weakly magnetic matrix is placed in a magnetic field, the magnetic spins of the particulates tend to align with the field. This increase in magnetic order lowers

the magnetic entropy of the spin system. If this process is performed adiabatically (i.e., no heat is exchanged with the surroundings), the reduction in spin entropy is offset by an increase in lattice entropy, and the specimen temperature will rise. This temperature rise is reversible (the specimen cools down on removal of the magnetic field) and is known as the magnetocaloric effect. Shull et al. [105] have shown that the nanocomposite $Gd_3Ga_{5-x}Fe_xO_{12}$ gives superior magnetocaloric effects which increase with x up to $x = 2.5$ and can be extended to higher temperatures than existing paramagnetic refrigerants. They have extensively investigated this phenomenon and predicted that the magnetocaloric effect may be enhanced at low fields and high temperatures.

6.6. Chemical properties

The corrosion behavior of nanocrystalline nickel-base alloys has been reported [106]. As expected, the average dissolution rate of Ni was found to be higher than that for the coarse-grained material. However, the nanocrystalline materials exhibited more uniform corrosion morphology in an acidic medium (the coarse-grained material suffered excessive intergranular corrosion) and superior localized corrosion resistance, attributed to the fine grain size and homogeneity of the nanocrystalline material.

Since majority of the synthesis methods produce nanocrystalline materials in a powder form, the total surface area available can be accurately controlled by controlling the particle size and porosity in the samples. One can consolidate the material to full density for best mechanical properties, or to a highly porous structure to obtain a large surface area, or to an intermediate value of porosity. Beck and Siegel [107] have shown that the chemical reactivity of nanocrystalline TiO_2 that has been only lightly consolidated is significantly higher than that in other commercially available TiO_2 samples. Nanocrystalline samples do not only have the increased activity, but the high activity is retained for a longer time than in commercial coarse-grained samples. This has been attributed to the large surface area of the nanocrystalline material combined with its rutile structure and its oxygen-deficient composition.

There has been an increased activity in this area recently [108–110]. A new class of Pd–Fe alloy, showing continuous solid solubility at all compositions, was shown to have a high degree of H_2 permeation through the membrane material, without experiencing poisoning by CO, H_2S, and H_2O, which is commonly encountered in membrane materials that are used for H_2 separation. Hydrogen absorbing alloys (FeTi, $LaNi_5$, Mg_2Ni, and other Mg-based materials) in the nanocrystalline form show much better hydrogen sorption properties than their polycrystalline counterparts. Further improvement was accomplished by modifying the metal powders with a small amount (<1 wt.%) of a catalyst, such as Pd, present in the form of small clusters or particles dispersed on the surface of the absorbing material [108].

There appears to be a lot of potential in developing improved catalytic materials for the industry. By controlling the processing parameters during the synthesis/production of nanocrystalline materials, one can fine-tune various crystalline structural parameters such as lattice parameters, defect concentration, surface chemistry, and compositional

variation. Further, one can control the structure of not only the catalytic material, but also their support. The nanoporous support design could further enhance the overall catalytic processes through increased activity, better selectivity, improved stability, and greater poisoning resistance [110].

7. Applications

Nanocrystalline materials are relatively new and it is only during the past few years that researchers have started exploring the many potential benefits of these materials. Several potential applications have been suggested based on the special attributes of these materials. It is most unlikely that the applications of these materials are decided on the basis of any one single property, but will be based mostly on the combination of a number of desirable properties. Currently, bulk nanostructured soft magnetic iron-based alloys and WC–Co nanocomposites have found industrial uses [40]. The different applications of nanocrystalline materials will be discussed under the groups of structural, magnetic, and chemical applications.

7.1. Structural applications

It has been known that the fracture toughness of ceramics can be considerably enhanced by dispersing in them a second phase on a microscopic scale. Since reducing the grain size to nanometer dimensions can provide increased strength and hardness, it is suggested that fabrication of micro/nanohybrids will lead to a new class of superstrong and supertough ceramics. In these hybrids, a nanocomposite matrix is reinforced with submicrometer-sized particles – whiskers, platelets, or long fibers – and these hybrids show enhanced fracture toughness and strength up to very high temperatures; the properties of coarse-grained composites normally degrade. Further, nanoreinforcements increase the creep resistance by suppressing grain boundary sliding. Consequently, nanoreinforcements are now being used to boost the performance of a growing number of composites. Nanoparticles of SiC markedly improve the fracture toughness and hardness of MgO/SiC composites developed by Mitsubishi Mining & Cement Co., Ltd., Japan. Nanocrystalline fibers also are used to reinforce composites. Nextel 610, a polycrystalline Al_2O_3 fiber developed by 3M has a grain size of 100 nm and strength of 2.4 GPa [111]. Microstructure of the mullite-based 3M fiber is a two-phase nanocomposite of 55% mullite and 45% Al_2O_3 by weight, with 20% 200-nm mullite needles randomly dispersed in a matrix of 100-nm Al_2O_3 particles. The fiber retains 85% of its tensile strength at 1200°C [112]. Such superceramics may find use in severe engineering applications such as high efficiency gas turbines, and in aerospace and automotive components.

It has been shown [113] that the hardness of WC–Co composites with nanometered WC grains increases with decreasing Co content and decreasing grain size, reaching values as high as 2,200 VHN. Scratch tests suggested that the higher hardness in nanograined WC–Co is also accompanied by increased toughness. Thus, the abrasive

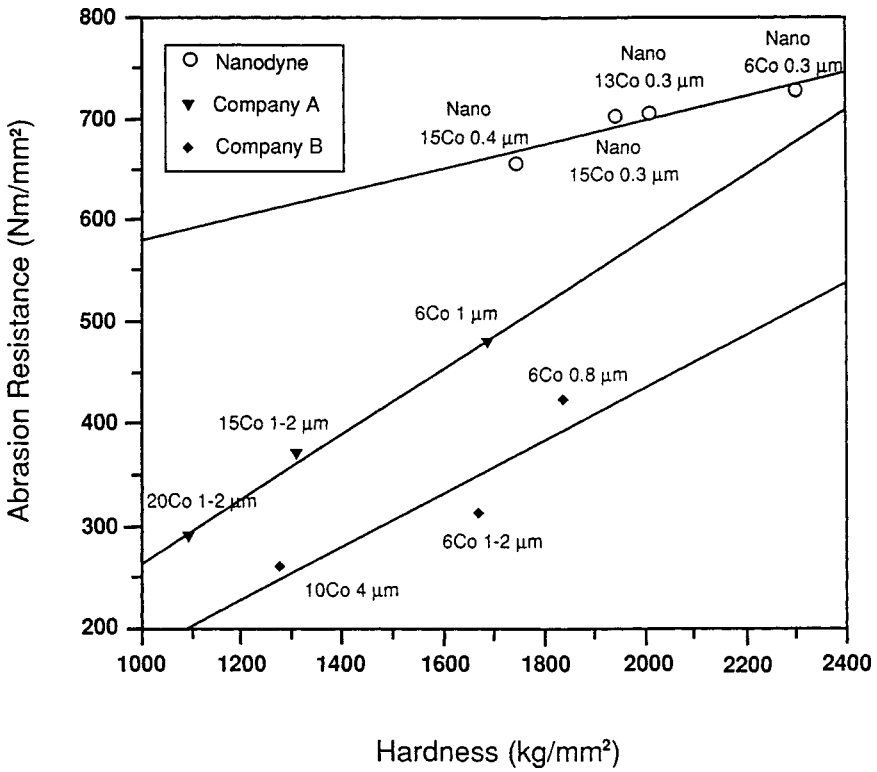

Figure 8. Abrasion resistance versus hardness of conventional and nanocrystalline WC–Co materials.

wear resistance of nanostructured WC–Co is higher than the abrasive wear resistance of conventional WC–Co when the comparison is made at equal hardness (figure 8). Thus, nanocrystalline WC–Co cutting tools are expected to have more than double lifetime than conventional coarse-grained composites. It has also been suggested that these could be used as fine drill bits for drilling holes in printed circuit boards and as rotary cutting tools (because of the fine grain size, sharp edges, and smooth surface finish).

Ontario Hydro Technologies developed the Electrosleeve steam generator tube repair technology based on bulk nanostructured deposits [33]. This *in-situ* repair technology involves the application of an internal sleeve in the area of the tubesheet to effect a complete pressure boundary restoration of degraded tubing. The technology produces a nanostructured nickel microalloy sleeve (several hundred microns thick) having a continuous high strength metallurgical bond to the steam generator tube, superior strength and ductility, and resistance to wear, fatigue and corrosion. The Electrosleeve was found to significantly outperform other commercially available repair technologies.

The improved hardness and strength coupled with better corrosion and wear resistance of nanocrystalline electrodeposits makes them strong contenders for protective coating applications [33]. These materials can be used as hard facing on softer, less wear-resistant substrates to improve the life-time resulting in cost savings. A nanocrys-

talline nickel coating on Nd–Fe–B hard magnets provided the required wear and corrosion resistance. Because of the small grain size and increased phonon scattering at grain and layer boundaries, nanocrystalline thermal barrier coatings should adhere better and at the same time exhibit reduced thermal conductivity [114]. One can also deposit nanocrystalline coatings to improve the wear-resistance while retaining a tough interior for low-temperature applications.

Nanocrystalline coatings deposited by laser plasma discharge increased the life of ZnS samples more than five times against abrasion/erosion/rain water corrosion/impact damage [115]. A double layer coating has been found to be a suitable method to improve the mechanical properties and recording characteristics of amorphous-ultrafine thin films; controlling the polymer coating thickness is still a problem.

Multilayered nanoscale structures also have superior sliding wear resistance at low loads compared to their coarse-grained counterparts.

7.2. Magnetic applications

The electrical and magnetic properties of nanocrystalline materials will probably form the basis for their widespread and industrial applications. A new class of electrically conducting, diamond-like nanocomposites with conductivity varying over 18 orders of magnitude have been synthesized. Extremely stable metal–dielectric multilayer structures without interfacial structural boundaries have also been fabricated. The unique combination of diamond-like chemical and mechanical properties with high electrical conductivity could lead to applications in the semiconductor and microelectronics industries as well as in battery technology. The phenomenon of giant magnetoresistance (GMR) can be used for the recording heads of the next generation of information storage systems.

In the area of permanent magnet materials, an exciting new development is that dealing with exchange coupled magnets. In these magnets there is an excess of α-Fe (up to 40 vol %) which couples to the hard magnetic phase, either $Nd_2Fe_{14}B$ or $Sm_2Fe_{17}N_3$. There is now a large market for strong rare-earth based permanent magnets in a wide variety of applications, and flexibility in manufacturing and lower material costs (less expensive rare-earth metals needed in remanence enhanced magnets) should encourage use of nanostructured materials.

The exceptional soft magnetic properties of the “FINEMET” and “Nanoperm” nanocrystalline/amorphous Fe-base alloys promise applications in transformer cores for power frequencies, saturable reactors, high-frequency transformers, and magnetic heads. Additional probable applications are for data communication interface components (pulse transformers), sensors (current transformers, magnetic direction sensors), common mode choke coils, and magnetic shielding. The phenomenon of magnetocaloric effect can be used for magnetic refrigeration, avoiding the use of harmful chlorofluorocarbons.

Magnetic recording materials to some extent already use nanostructured materials. Magnetic materials are used in both the information storage media and in the “write” and

"read" heads. It is predicted that in the future essentially all media and heads will contain nanostructured materials [116]. Thin film recording media (e.g., disks) typically have thickness of 10–100 nm and at very high bit densities, longitudinal media must be very thin (10–50 nm) while perpendicular recording media can be much thicker (50–250 nm) [117]. These films are mainly prepared by sputtering of Co-based alloys. In particulate media (e.g., tapes) the structure for high-density applications consists of an acicular iron core passivated by an oxide surface. The iron particles are about 200 nm long and about 20 nm in diameter [118]. For both particulate and film media the magnetic single domains must become even smaller to achieve higher densities with satisfactory signal-to-noise ratios – but not so small as to become paramagnetic.

7.3. Chemical applications

The large surface area of nanocrystalline materials can be used for catalysis purposes. It has been shown in several studies that the catalytic activity and selectivity can be dependent on particle size. Beck and Siegel [107] showed that the chemical reactivity of nanocrystalline TiO_2 that was only partly consolidated to maximize porosity, and therefore surface area, is much higher than in other commercially available TiO_2. Figure 9 shows the catalytic activity for S removal from H_2S by decomposition for several forms of TiO_2 with different crystal structures (rutile or anatase) and surface areas. The greater activity of the nanocrystalline TiO_2 samples was attributed to its crystal structure (rutile), its high surface area, and its oxygen deficient composition. Vitulli et al. [119] observed a strong correlation between Pt particle sizes and catalytic activity. That is, very small Pt particles (3–6 nm) showed an unusual catalytic activity in the hydrogenation of p-chloronitrobenzene. Commercial catalysts with about 20 nm Pt particles only promote the catalytic reduction of the NO_2 group while the small (3–6 nm) Pt particles catalyze the unusual formation of dicyclohexylamine 8 in large quantity. However, the electronic structure of metal nanocrystallites supported on oxides suggests no change from bulk behavior even down to 1 nm for Pt, Ir, or Os [120]. Furthermore, it cannot be assured that the integrity of a nanocrystallite – its composition and position – will remain in tact when it is used for a catalyst [121].

Metal hydrides offer the best compromise of safety, efficiency, and cost for storage of hydrogen for use as a fuel. Unfortunately their use is hindered by the sensitivity of their kinetic properties to surface oxidation. Hydrides of intermetallic compounds need activation treatments – often at elevated temperatures and pressures – after exposure to air. It was believed that a way to enhance their properties is to produce the materials in nanocrystalline form. The high density of grain boundaries/interfaces might increase diffusion. Nanocrystalline $Fe_{40}Ti_{60}$ and $Fe_{50}Ti_{50}$ exhibited, compared to coarse-grained alloys, increased solubility at low pressure, narrowing of the miscibility gap, lower plateau pressure, and disappearance of the transformation to γ-$FeTiH_{1.90}$ [122]. Nanocrystalline Mg_2Ni inclusions in a two-phase Mg/Mg_2Ni alloy showed improved hydrogen storage behavior in terms of the Mg_2Ni catalyzing the decomposition of the molecular hydrogen, greatly increasing the hydrogen absorption/desorption kinetics [123]. A further advan-

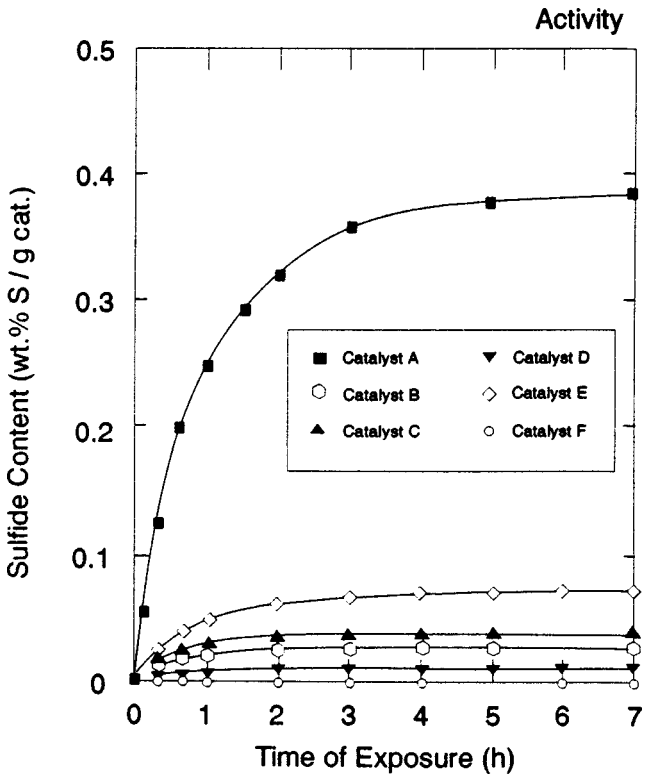

Figure 9. Activity of nanocrystalline TiO_2 for H_2S decomposition as a function of exposure time at 500°C compared with that from several commercial TiO_2 materials and a reference.

tage of the nanoscale microstructure is that the alloy powder does not comminute as the result of repeated hydrogen charging–discharging cycles.

8. Concluding remarks

Nanocrystalline materials are novel materials that are not only scientifically interesting but also hold great potential for a number of technological applications. Their properties are different from and often superior to those of conventional coarse-grained polycrystalline materials and also amorphous alloys of the same composition.

Widespread use and search for technological applications of nanocrystalline materials requires the availability of large (tonnage) quantities of well-characterized material with reproducible properties; and this needs to be done economically. Even though nanocrystalline powders are now more expensive than the more commercially available coarse-grained powders, greater usage and tonnage production will bring down the cost. In this respect, one can recall the case of metallic glass tapes produced by the rapid solidification processing, now being used commercially for transformer core laminations. While the tapes costed US$ 300 per kg in late 1978 when they were first produced they

now cost only about $2 [124]. A solution to the barriers for commercial utilization of nanocrystalline materials can be identification of well-defined applications for these materials and this can be a driver for accelerated research. In this context, development of novel synthesis methods to produce these materials in commercially viable quantities is an urgent necessity. Simultaneously, the properties of the existing materials need to be significantly improved. Further studies on nanoglasses, nano-quasicrystalline alloys, and nanocomposites are required to evaluate the properties and compare these with the nanocrystalline alloys. Applications of nanostructured materials are in their infancy, but the explosion of interest in this field is expected to provide an early maturation.

References

[1] C. Suryanarayana, Inter. Mater. Rev. 40 (1995) 41.
[2] J.M. Silcock, T.J. Heal and H.K. Hardy, J. Inst. Metals 82 (1953–54) 239.
[3] J.B. Cohen, Metall. Trans. 23A (1992) 2685.
[4] R.M. Scanlan, W.A. Fietz and E.F. Koch, J. Appl. Phys. 46 (1975) 2244.
[5] A.A. Voevodin, S.V. Prasad and J.S. Zabinski, J. Appl. Phys. 82 (1997) 855.
[6] H. Gleiter, Prog. Mater. Sci. 33 (1989) 223.
[7] R. Uyeda, Prog. Mater. Sci. 35 (1991) 1.
[8] R.W. Siegel, in: *Processing of Metals and Alloys*, Materials Science and Technology – A Comprehensive Treatment, Vol. 15, ed. R.W. Cahn (VCH, Weinheim, Germany, 1991) p. 583.
[9] R.W. Siegel, NanoStruct. Mater. 4 (1994) 121.
[10] H. Gleiter, NanoStruct. Mater. 6 (1995) 3.
[11] C. Suryanarayana and C.C. Koch, in: *Non-Equilibrium Processing of Materials*, ed. C. Suryanarayana (Elsevier Science, Oxford, UK, 1999) p. 313.
[12] C.C. Koch and C. Suryanarayana, in: *Microstructure and Properties of Materials*, Vol. 2, ed. J.C.M. Li (World Scientific Publishing Corp., Singapore, 2000) p. 359.
[13] R.D. Shull and J.M. Sanchez eds., *Nanophases and Nanocrystalline Structures* (TMS, Warrendale, PA, 1993).
[14] G.C. Hadjipanayis and R.W. Siegel, eds., *Nanophase Materials: Synthesis, Properties, Applications* (Kluwer Academic Publishers, Dordrecht, The Netherlands, 1994).
[15] C. Suryanarayana, J. Singh and F.H. Froes, eds., *Processing and Properties of Nanocrystalline Materials* (TMS, Warrendale, PA, 1996).
[16] D.L. Bourell, ed., *Synthesis and Processing of Nanocrystalline Powder* (TMS, Warrendale, PA, 1996).
[17] A.S. Edelstein and R.C. Cammarata, eds., *Nanomaterials: Synthesis, Properties, and Applications* (Inst. Physics, Bristol, UK, 1996).
[18] E. Ma, B. Fultz, R.D. Shull, J. Morral and P. Nash, eds., *Chemistry and Physics of Nanostructures and Related Non-Equilibrium Materials* (TMS, Warrendale, PA, 1997).
[19] C. Suryanarayana and F.H. Froes, Metall. Trans. 23A (1992) 1071.
[20] K. Lu, Mater. Sci. Eng. Reports R 16 (1996) 161.
[21] R.W. Siegel, MRS Bulletin 15(10) (1990) 60.
[22] C.G. Granqvist and R.A. Buhrman, J. Appl. Phys. 47 (1976) 2200.
[23] H. Konrad, T. Haubold, R. Birringer and H. Gleiter, NanoStruct. Mater. 7 (1996) 605.
[24] W. Chang, G. Skandan, S.C. Danforth, B.H. Kear and H. Hahn, NanoStruct. Mater. 4 (1994) 507.
[25] C.C. Koch, NanoStruct. Mater. 2 (1993) 109; and 9 (1997) 13.
[26] C. Suryanarayana, Prog. Mater. Sci. 46 (2001) 1.

[27] R.Z. Valiev, in: *Nanophase Materials: Synthesis, Properties, Applications*, eds. G.C. Hadjipanayis and R.W. Siegel (Kluwer Academic Publishers, Dordrecht, The Netherlands, 1994) p. 275; NanoStruct. Mater. 6 (1995) 73.
[28] Y. Saito, H. Utsunomiya, N. Tsuji and T. Sakai, Acta Mater. 47 (1999) 579.
[29] B.H. Kear and L.E. McCandlish, NanoStruct. Mater. 3 (1993) 19; B.H. Kear and P.R. Strutt, NanoStruct. Mater. 6 (1995) 227.
[30] U. Erb, NanoStruct. Mater. 6 (1995) 533.
[31] I. Bakonyi, E. Toth-Kadar, J. Toth, T. Tarnoczi and A. Cziraki, in: *Processing and Properties of Nanocrystalline Materials*, eds. C. Suryanarayana et al. (TMS, Warrendale, PA, 1996) p. 465.
[32] D.S. Lashmore and M.P. Dariel, in: *Encyclopedia of Materials Science and Engineering*, ed. R.W. Cahn (Pergamon Press, Oxford, UK, 1988) suppl. Vol. 1, p. 136.
[33] C. Cheung, D. Wood and U. Erb, in: *Processing and Properties of Nanocrystalline Materials*, eds. C. Suryanarayana et al. (TMS, Warrendale, PA, 1996) p. 479.
[34] Y. Yoshizawa, S. Oguma and K.J. Yamauchi, J. Appl. Phys. 64 (1988) 6044.
[35] K. Lu, in: *Processing and Properties of Nanocrystalline Materials*, eds. C. Suryanarayana et al. (TMS, Warrendale, PA, 1996) p. 23.
[36] U. Köster, Mater. Sci. Forum 235–238 (1997) 377.
[37] M.L. Trudeau, in: *Nanophase Materials: Synthesis, Properties, Applications*, eds. G.C. Hadjipanayis and R.W. Siegel (Kluwer Academic Publishers, Dordrecht, The Netherlands, 1994) p. l53.
[38] R.L. Bickerdike, D. Clark, J.N. Easterbrook, G. Hughes, W.N. Mair, P.G. Partridge and H.C. Ranson, Internat. J. Rapid Solidification 1 (1984–85) 305.
[39] G. Liu, Adv. Mater. 9 (1997) 437.
[40] M.N. Rittner and T. Abraham, JOM 50(1) (1998) 36.
[41] K. Okazaki, in: *Advanced Synthesis of Engineered Structural Materials*, eds. J.J. Moore et al. (ASM International, Materials Park, OH, 1993) p. 197.
[42] M.J. Mayo, Internat. Mater. Rev. 41 (1996) 85.
[43] R.J. Dowding, J.J. Stiglich and T.S. Sudarshan, in: *Advances in Powder Metallurgy & Particulate Materials – 1994*, Vol. 5, eds. C. Lall and A.J. Neupaver (Metal Powder Industries Federation, Princeton, NJ, 1994) p. 45.
[44] J.R. Groza, in: *Non-Equilibrium Processing of Materials*, ed. C. Suryanarayana (Elsevier Science, Oxford, UK, 1999) p. 347.
[45] C. Suryanarayana and G.E. Korth, Met. and Mater. 5 (1999) 121.
[46] G.W. Nieman and J.R. Weertman, in: *Proc. M.E. Fine Symposium*, eds. P.K. Liaw et al. (TMS, Warrendale, PA, 1991) p. 243.
[47] J. Weismüller, J. Löfler, C. Krill, R. Birringer and H. Gleiter, in preparation; quoted in [54].
[48] X.D. Liu, K. Lu, B.Z. Ding and Z.Q. Hu, NanoStruct. Mater. 2 (1993) 581.
[49] M.L. Sui and K. Lu, Mater. Sci. Eng. A179–180 (1994) 541.
[50] X.D. Liu, H.Y. Zhang, K. Lu and Z.Q. Hu, J. Phys. C 6 (1994) L497.
[51] H.Y. Zhang, K. Lu and Z.Q. Hu, J. Phys. C 7 (1995) 5327.
[52] D. Chen, NanoStruct. Mater. 4 (1994) 753.
[53] K. Kimoto and I. Nishida, J. Phys. Soc. Jap. 22 (1967) 744.
[54] J. Weismüller, in: *Synthesis and Processing of Nanocrystalline Powder*, ed. D.L. Bourell (TMS, Warrendale, PA, 1996) p. 3.
[55] J. Weismüller, J. Löfler and M. Kebler, NanoStruct. Mater. 6 (1995) 105.
[56] R. Birringer, in: *Nanophase Materials: Synthesis, Properties, Applications*, eds. G.C. Hadjipanayis and R.W. Siegel (Kluwer Academic Publishers, Dordrecht, The Netherlands, 1994) p. 157.
[57] R.W. Siegel, in: *Materials Interfaces: Atomic Level Structure and Properties*, eds. D. Wolf and S. Yip (Chapman & Hall, London, UK, 1992) p. 431.
[58] H. Ouyang, B. Fultz and H. Kuwano, in: *Nanophases and Nanocrystalline Structures*, eds. R.D. Shull and J.M. Sanchez (TMS, Warrendale, PA, 1993) p. 95.

[59] S.R. Phillpot, D. Wolf and H. Gleiter, J. Appl. Phys. 78 (1995) 847.
[60] Z. Horita, D.J. Smith, M. Furukawa, M. Nemoto, R.Z. Valiev and T.G. Langdon, J. Mater. Res. 11 (1996) 1880.
[61] D.H. Ping, D.X. Li and H.Q. Ye, J. Mater. Sci. Lett. 14 (1995) 1536.
[62] T.R. Malow and C.C. Koch, in: *Synthesis and Processing of Nanocrystalline Powder*, ed. D.L. Bourell (TMS, Warrendale, PA, 1996) p. 33.
[63] B. Günther, A. Kumpmann and H.D. Kunze, Scripta Metall. Mater. 27 (1992) 833.
[64] J. Eckert, J.C. Holzer and W.L. Johnson, J. Appl. Phys. 73 (1993) 131.
[65] T.R. Malow and C.C. Koch, Acta Mater. 45 (1997) 2177.
[66] V.Y. Gertsman and R. Birringer, Scripta Metall. Mater. 30 (1994) 577.
[67] C.E. Krill, R. Klein, S. Janes and R. Birringer, Mater. Sci. Forum 179–181 (1995) 443.
[68] H. Hahn, J. Logas and R.S. Averback, J. Mater. Res. 5 (1990) 609.
[69] J. Horvath, Defect & Diff. Forum 66–69 (1989) 207.
[70] S. Schumacher, R. Birringer, R. Strauss and H. Gleiter, Acta Metall. 37 (1989) 2485.
[71] B.S. Bokstein, H.D. Bröse, L.I. Trusov and T.P. Khvostantseva, NanoStruct. Mater. 6 (1995) 873.
[72] E. Ivanov, Mater. Sci. Forum 88–90 (1992) 475.
[73] R.W. Siegel and H. Hahn, in: *Current Trends in the Physics of Materials*, ed. M. Youssouff (World Sci. Pub. Co., Singapore, 1987) p. 403.
[74] J. Karch, R. Birringer and H. Gleiter, Nature 330 (1987) 556.
[75] M.S. Choudry, J.A. Eastman, R.J. DiMelfi and M. Dollar, Scripta Mater. 37 (1997) 843.
[76] K. Lu and M.L. Sui, Acta Metall. Mater. 43 (1995) 3325.
[77] T. Turi and U. Erb, Mater. Sci. & Eng. A204 (1995) 34.
[78] E. Hellstern, H.J. Fecht, Z. Fu and W.L. Johnson, J. Appl. Phys. 65 (1989) 305.
[79] H.Y. Bai, L. Luo, D. Jin and J.R. Sun, J. Appl. Phys. 79 (1996) 361.
[80] M.L. Steigerwald and L.E. Brus, Ann. Rev. Mater. Sci. 19 (1989) 471.
[81] G. Skandan, H. Hahn and J.C. Parker, Scripta Metall. Mater. 25 (1991) 2389.
[82] G.D. Stucky and J.E. MacDougall, Science 27 (1990) 669.
[83] D.G. Morris, in: *Mechanical Properties of Nanostructured Materials*, Materials Science Foundations, Vol. 2 (Trans. Tech. Publ., Zürich, Switzerland, 1998).
[84] L. Wong, D. Ostrander, U. Erb, G. Palumbo and K.T. Aust, in: *Nanophases and Nanocrystalline Structures*, eds. R.D. Shull and J.M. Sanchez (TMS, Warrendale, PA, 1993) p. 85.
[85] T.D. Shen, C.C. Koch, T.Y. Tsui and G.M. Pharr, J. Mater. Res. 10 (1995) 2892.
[86] A.M. El-Sherik, U. Erb, V. Krstic, B. Szpunar, M.J. Aus, G. Palumbo and K.T. Aust, MRS Symp. Proc. 286 (1993) 173.
[87] C.C. Koch, D.G. Morris, K. Lu and A. Inoue, MRS Bulletin 24(2) (1999) 54.
[88] P.G. Sanders, M. Rittner, E. Kiedaisch, J.R. Weertman, H. Kung and Y.C. Lu, NanoStruct. Mater. 9 (1997) 433.
[89] A. Inoue, N. Nakazato, Y. Kawamura and T. Masumoto, Mater. Sci. & Eng. A179/180 (1994) 654.
[90] S.X. McFadden, R.S. Mishra, R.Z. Valiev, A.P. Zhilyaev and A.K. Mukherjee, Nature 398 (1999) 684.
[91] R.W. Siegel, Mater. Sci. Forum 235–238 (1997) 851.
[92] K. Lu, Y.Z. Wang, W.D. Wei and Y.Y. Li, Adv. Cryog. Mater. 38 (1991) 285.
[93] X.D. Liu, B.Z. Ding, Z.Q. Hu, K. Lu and Y.Z. Wang, Physica B 192 (1993) 345.
[94] X.D. Liu, J.T. Wang and B.Z. Ding, Scripta Metall. Mater. 28 (1993) 59.
[95] J.T. Lee, J.H. Hwang, J.J. Mashek, T.O. Mason, A.E. Miller and R.W. Siegel, J. Mater. Res. 10 (1995) 2295.
[96] R.N. Viswanath, S. Ramasamy, R. Ramamoorthy, P. Jayavel and T. Nagarajan, NanoStruct. Mater. 6 (1995) 993.
[97] R.H. Yu, X.X. Zhang, J. Tejada, M. Knobel, P. Tiberto and P. Allia, J. Phys. D 28 (1995) 1770.
[98] C.E. Krill, F. Merzoug, W. Krauss and R. Birringer, NanoStruct. Mater. 9 (1997) 455.

[99] U. Erb, G. Palumbo, B. Szpunar and K.T. Aust, NanoStruct. Mater. 9 (1997) 261.
[100] G. Herzer, Scripta Metall. Mater. 33 (1995) 1741.
[101] A. Makino, A. Inoue and T. Masumoto, NanoStruct. Mater. 6 (1995) 985.
[102] A. Makino, A. Inoue and T. Masumoto, Mater. Trans. Jpn. Inst. Metals 36 (1995) 924.
[103] L. Schultz, J. Wecker and E. Hellstern, J. Appl. Phys. 61 (1987) 3583.
[104] P.A.I. Smith, J. Ding, R. Street and P.G. McCormick, Scripta Mater. 34 (1996) 61.
[105] R.D. Shull, R.D. McMichael and J.J. Ritter, NanoStruct. Mater. 2 (1993) 205.
[106] R. Rofagha, U. Erb, D. Ostrander, G. Palumbo and K.T. Aust, NanoStruct. Mater. 2 (1993) 1.
[107] D.D. Beck and R.W. Siegel, J. Mater. Res. 7 (1992) 2840.
[108] L. Zaluski, A. Zaluska, P. Tessier, J.O. Ström-Olsen and R. Schulz, Mater. Sci. Forum 225–227 (1996) 853.
[109] K.Z. Chen, Z.K. Zhang, Z.L. Cui, D.H. Zuo and D.Z. Yang, NanoStruct. Mater. 8 (1997) 205.
[110] M.L. Trudeau and J.Y. Ying, NanoStruct. Mater. 7 (1996) 245.
[111] G. Das, Ceram. Eng. & Sci. Proc. 17 (1996) 25.
[112] Adv. Mater. Proc. 146(4) (1994) 25.
[113] L.E. McCandlish, V. Kevorkian, K. Jia and T.E. Fischer, in: *Advances in Powder Metallurgy & Particulate Materials – 1994*, Vol. 5, eds. C. Lall and A.J. Neupaver (Metal Powder Industries Federation, Princeton, NJ, 1994) p. 329.
[114] M. Gell, Mater. Sci. & Eng. A 204 (1995) 246.
[115] F. Davanloo, T.J. Lee, H. Park, J.H. You and C.B. Colins, J. Mater. Res. 8 (1993) 3090.
[116] A. Berkowitz, in: *Nanomaterials: Synthesis, Properties, and Applications*, eds. A.S. Edelstein and R.C. Cammarata (Institute of Physics, Bristol, 1996) p. 569.
[117] J.H. Judy, MRS Bulletin 15(3) (1990) 63.
[118] M.P. Sharrock, MRS Bulletin 15(3) (1990) 53.
[119] G. Vitulli, E. Pitzalis, A. Verrazzani, P. Pertici, P. Salvadori and G. Martra, Mater. Sci. Forum 235–238 (1997) 929.
[120] J.H. Sinfelt and G.D. Meitzner, Accounts Chem. Res. 26 (1993) 1.
[121] D.R. Rolison, in: *Nanomaterials: Synthesis, Properties, and Applications*, eds. A.S. Edelstein and R.C. Cammarata (Institute of Physics, Bristol, 1996) p. 305.
[122] P. Tessier, L. Zaluski, A. Zaluska, J.O. Ström-Olsen and R. Schulz, Mater. Sci. Forum 225–227 (1996) 869.
[123] M.L. Wasz, R.B. Schwarz, S. Srinivasan and M.P.S. Kumar, Mater. Res. Soc. Symp. Proc. 393 (1995) 237.
[124] C.H. Smith, in: *Rapidly Solidified Alloys: Processes, Structures, Properties, Applications*, ed. H.H. Liebermann (Marcel-Dekker, New York, 1993) p. 617.